Consecutive Bright Pulses in the Vela Pulsar

Jim Lindley Palfreyman B.Sc. (Hons)

Submitted in fulfilment of the requirements for the degree of

Master of Science

University of Tasmania

October 2012

Abstract

We report on the discovery of consecutive bright radio pulses from the Vela pulsar, a new phenomenon that may lead to a greater understanding of the pulsar emission mechanism. This results from a total of 345 hours worth of observations of the Vela pulsar using the University of Tasmania's 26 m radio telescope to study the frequency and statistics of abnormally bright pulses and sub-pulses. The bright pulses show a tendency to appear consecutively. The observations found two groups of six consecutive bright pulses and many groups of two to five bright pulses in a row. The strong radio emission process that produces the six bright pulses lasts between 0.4 and 0.6 seconds. The numbers of bright pulses in sequence far exceed what would be expected if individual bright pulses were independent random events. Consecutive bright pulses must be generated by an emission process that is long-lived relative to the rotation period of the neutron star.

We also confirm the existence of giant micro pulses previously observed in Vela, and also the apparent change in bright pulse occurrences after a glitch.

Dedication

This thesis is dedicated to my dad, Bob Palfreyman, who died suddenly during its writing. His lifelong love of astronomy and building of a kit Newtonian telescope when I was aged 10 kick-started me into the sciences.

Acknowledgments

First thanks go to my supervisors Professor John Dickey and Dr Aidan Hotan who have provided me with all the guidance, support, encouragement and direction I have needed. Science is all about standing on the shoulders of giants and building on previous work, and it has been a pleasure working with these two. They questioned my hunches and made me dig deeper where I needed to dig – just to make sure.

Next I'd like to thank the support team at Mt Pleasant, in particular Brett Reid and Eric Baynes for taking my weekend or late night calls, willing to help when something broke down and always with a smile.

I'd like to thank Tim Young for assisting in observations on the 2009 "100 hour" campaign and Claire Trenham for verifying some of my mathematics.

Willem van Straten provided me with what turned out to be an extremely valuable hour's worth of single pulse Vela data from the Parkes 64 m telescope. His encouragement, thoughts, and ideas for this project were most welcome.

I'd also like to thank my mum Jennie Clarke and my aunt Wendy Weight for the non-scientific proof reading.

Finally, I'd like to thank my partner Zonia Bell. She had to put up with late night and weekend visits to the telescope ("your other woman"), not to mention her support when Dad died, and of course the final and painful stretch of thesis writing.

Declaration

This thesis contains no material which has been accepted for a degree or diploma by the University or any other institution, except by way of background information, and duly acknowledged in the thesis, and to the best of the my knowledge and belief no material previously published or written by another person except where due acknowledgement is made in the text of the thesis; nor does the thesis contain any material that infringes copyright. All unattributed photos are by the author.

The published paper by Palfreyman, et al. (2011) that appeared in **Astrophysical Journal Letters** forms a major portion of this thesis – in particular Chapter 5. The publishers of that content hold copyright, and access to the material should be sought from the respective journal. The remaining non-published content of the thesis may be made available for loan and limited copying and communication in accordance with the Copyright Act 1968.

The author also provided data and was a co-author in:

Pellizzoni, A., et al. (2009) in the **Astrophysical Journal** titled "*Detection of Gamma-Ray Emission from the Vela Pulsar Wind Nebula with AGILE"*

Pellizzoni, A., et al. (2010) in **Science** titled "*High-Resolution Timing Observations of Spin-Powered Pulsars with the AGILE Gamma-Ray Telescope"*

Abadie, J., et al. (2011) in the **Astrophysical Journal** titled "*Beating the Spin-Down Limit on Gravitational Wave Emission from the Vela Pulsar*"

Contents

1. Introduction 11

1.1. Discovery of pulsars 11

1.2. Thesis Outline 12

2. An Introduction to Pulsar Astronomy 14

2.1. The Pulsar as a Lighthouse 14

2.2. Frequency and Period 18

2.3. Location of Pulsars Within the Galaxy 21

2.4. Light Cylinder and Polar Cap 22

2.5. Interstellar Medium 23

2.6. Glitches 25

2.7. Definitions 26

2.8. Giant Pulses in the Crab Pulsar 28

2.9. Vela Supernova Remnant and PSR J0835-4510 30

3. Emission Mechanisms and Bright Pulses 31

3.1. Emission 31

3.2. Drifting Sub-pulses 34

3.3. A Different Approach 37

4. Instrumentation, Software, and Data Collection 39

4.1. Mount Pleasant 39

4.2. Parkes 41

4.3. Analysis 42

4.4. Interference 43

4.5. Data Collected and Archiving 44

4.6. The Software Fault 45

4.7. The Glitch 46

5. Bright Pulses in PSR J0835-4510 47

5.1. Bright or Giant pulses? 47

5.2. Consecutive Bright Pulses and the Consequences for Emission Hypotheses 58

5.3. Parkes Data Confirmation 62

6. Confirmation of Giant Micro Pulses 72

7. Glitches and their possible Effects on Bright Pulses 76

8. Conclusion 82

8.1. Summary 82

8.2. Future Work 85

9. References 86

List of Figures

Figure 1: The first pulsar pulses ever seen from CP1919 11

Figure 2: The Homunculus Nebula in Eta Carina from the Hubble Space Telescope. 14

Figure 3: Not-to-scale drawing of a pulsar and its surroundings. 16

Figure 4: Nested cone structure of Rankin (1993). 17

Figure 5: Patchy beam model of Lyne & Manchester (1988) 17

Figure 6: Micro structure and multiple peaks that can occur in a pulsar's pulse. 18

Figure 7: Histogram of log(period) of all known pulsars 19

Figure 8: Histogram of log(characteristic age) of known pulsars 21

Figure 9: Plot of all known pulsars by galactic latitude v longitude 22

Figure 10: The Crab supernova remnant from the Hubble Space Telescope 28

Figure 11: Diagram showing proposed emission layers and patches within those layers 32

Figure 12: Drifting sub pulses from B0943+10 from Deshpande & Rankin (1999) 35

Figure 13: Rotating carousel of emission centres from Deshpande & Rankin (1999) 36

Figure 14: Not-to-scale picture showing neutron star, magnetosphere, and gap 37

Figure 15: The 26 m radio telescope at Mt Pleasant near Hobart, Tasmania 39

Figure 16: The 64 m telescope at Parkes, NSW 41

Figure 17: Explanation of how Full Width Half Maximum (FWHM) is calculated 43

Figure 18: Mean pulse for Vela as observed at Mt Pleasant 48

Figure 19: Mean pulse for Vela as observed at Parkes. 48

Figure 20: The brightest pulse in our observing runs at Mt Pleasant 49

Figure 21: Magnified view of bright pulse in previous figure. 50

Figure 22: Microstructure for the brightest pulse recorded in the Mt Pleasant data. T-2. 51

Figure 23: Microstructure for the brightest pulse recorded in the Mt Pleasant data. T-1. 51

Figure 24: Microstructure for the brightest pulse recorded in the Mt Pleasant data. 52

Figure 25: Microstructure for the brightest pulse recorded in the Mt Pleasant data. T+1.....52

Figure 26: The first consecutive bright pulses discovered in our data. 54

Figure 27: Microstructure for the brightest pulse recorded in the Parkes data. T-3. 55

Figure 28: Microstructure for the brightest pulse recorded in the Parkes data. T-2. 55

Figure 29: Microstructure for the brightest pulse recorded in the Parkes data. T-1. 56

Figure 30: Microstructure for the brightest pulse recorded in the Parkes data. 56

Figure 31: Microstructure for the brightest pulse recorded in the Parkes data. T+1. 57

Figure 32: Microstructure for the brightest pulse recorded in the Parkes data. T+2. 57

Figure 33: Six consecutive bright pulses seen at 2008 June 29 07:32:20.9823 UTC. 58

Figure 34: Plot of flux density vs phase for each of the consecutive bright pulses.....59

Figure 35: Time vs time graph of the quadruple pulse recorded at Parkes. 63

Figure 36: Same as previous, but magnified.....64

Figure 37: Pulse 1 of 4 at 1249 MHz. 65

Figure 38: Pulse 2 of 4 at 1249 MHz. 65

Figure 39: Pulse 3 of 4 at 1249 MHz. 66

Figure 40: Pulse 4 of 4 at 1249 MHz. 66

Figure 41: Pulse 1 of 4 at 1441 MHz. 67

Figure 42: Pulse 2 of 4 at 1441 MHz. 67

Figure 43: Pulse 3 of 4 at 1441 MHz. 68

Figure 44: Pulse 4 of 4 at 1441 MHz. 68

Figure 45: Magnified view of potential Fraunhofer diffraction at 1249 MHz. 69

Figure 46: Magnified view of potential Fraunhofer diffraction at 1489 MHz. 70

Figure 47: Peak flux density vs width for bright pulses prior to July 31 2010 72

Figure 48: Scatterplot of peak flux density vs width for approximately 40000 pulses 74

Figure 49: Plot of all bright pulses and their peak flux density vs observation date.....78

Figure 50: Histogram of a count of bright pulses each observing minute 79

Figure 51: Histogram of bright pulses per observing minute before and after the glitch 79

Figure 52: Peak flux density vs pulse width for bright pulses observed after the glitch.....80

1.Introduction

1.1. Discovery of pulsars

In 1968 Jocelyn Bell, under the supervision of Professor Anthony Hewish discovered pulses on a chart recorder that at first looked to be of human origin. However since these pulses reappeared $23^h\ 56^m$ later each day the origin was unlikely to be terrestrial.

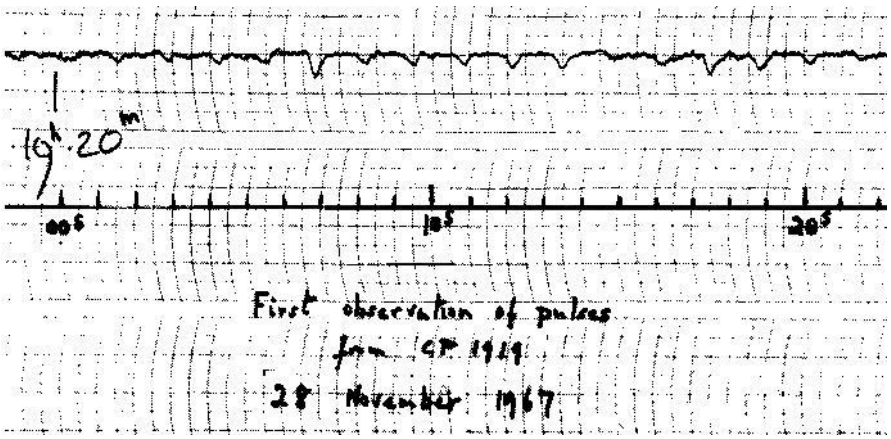

Figure 1: The first pulsar pulses ever seen from CP1919 (Hewish, Bell et al, 1968).

News spread rapidly and a hunt for other similar "pulsating stars" began. Soon after, a pulsar was discovered in the constellation Vela amongst a supernova remnant (Large, Vaughn & Mills 1968), and this was observed at Molonglo Observatory outside Canberra. The pulses were too rapid to measure their frequency on the chart recorder and so one pen was connected to 50Hz from the power point and another pen to the antenna. Since the chart recorder couldn't push the paper through fast enough, the operator sprinted down the hall, pulling the paper through the recorder as the pulsar passed overhead. With both traces on the paper they correctly identified the Vela pulsar period accurate to one decimal place – 89.3 ms. (Vaughan, 2008)

The discovery by Large, Vaughan & Mills of the Vela pulsar not only linked the creation of neutron stars to supernovae, but also discovered what turned out to be the “brightest” (in a radio sense) pulsar in the southern sky.

1.2. Thesis Outline

The focus of this research was “bright” pulses emitted by the Vela pulsar. It was well known that Vela emits occasional bright pulses, but no long-term single pulse studies had ever been performed. This study collected 345 hours of single pulse observations over 4 years for a total of over 10^7pulses. As of this writing it is believed to be the longest single pulse study in the world. It was noted early on that two bright pulses occasionally came consecutively. So a search was instigated for such occurrences. Whilst demonstrating the data to a visiting American researcher, a random file (known to contain at least one “multiple”) was displayed for demonstration purposes. It turned out to have 6 consecutive bright pulses! Even though the sequential search would eventually have found this, that moment set the outline for this research.

The appearance and number of these consecutive pulses will be shown to appear many orders of magnitude higher than if they were independent events. Other explanations for these will be ruled out and the consecutive bright pulses will be shown to have been emitted by the Vela pulsar. A brief survey of some of the key emission possibilities will be discussed and what this result means to those hypotheses.

Vela occasionally (every 2-4 years) speeds up briefly in rotation (colloquially called a “glitch”) and it will be noted that after the glitch that occurred in July 2010, the bright pulse

rate increased drastically. Also, the “giant micro pulses” that Johnston et al (2001) observed have been confirmed and will be discussed.

---

2. An Introduction to Pulsar Astronomy

2.1. The Pulsar as a Lighthouse

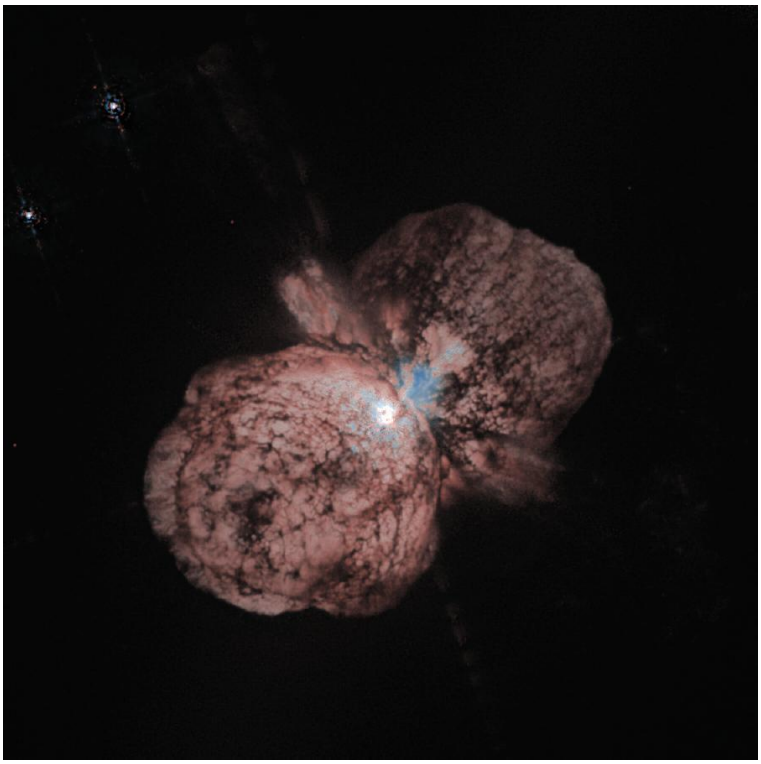

Figure 2: The Homunculus Nebula in Eta Carina from the Hubble Space Telescope. Photo Credit: Jon Morse (University of Colorado), and NASA

At the end of a sufficiently massive star's life (9 solar masses or more), a Type II supernova occurs and leaves behind a core that is crushed by intense gravity. Since the electron degeneracy pressure can no longer support it, the electrons are forced into the nucleus to combine with the protons to form neutrons. The size of the star shrinks rapidly to, on average, about 20 km in diameter (Lattimer & Prakash 2001) and 1.4 solar masses (Stairs, 2004). This material is on average extremely dense (6.7×10^{14} g cm^{-3}), but in reality has

different densities at different layers in the neutron star. Most models have a lighter density outer crust and a heavier density inner “sea” of superfluid neutrons (Pines & Alpar 1985).

If the original star was greater than 20 solar masses then the escape velocity exceeds the speed of light and a black hole is formed. However, the focus on this thesis is on those 9-20 solar mass stars that collapse to neutron stars.

As the star collapses, its typically slow rotation rate increases rapidly due to conservation of angular momentum. A neutron star is also an extremely strong magnet (typically 10^{11} to 10^{13} G) and the rotational axis does not necessarily line up with the magnetic axis. Figure 3 is a not-to-scale drawing of a pulsar, its magnetic field lines and its emission cones (which are from the magnetic poles). So if the line of sight from a pole passes over the Earth, a brief flash of electromagnetic radiation is seen - and we have a pulsar.

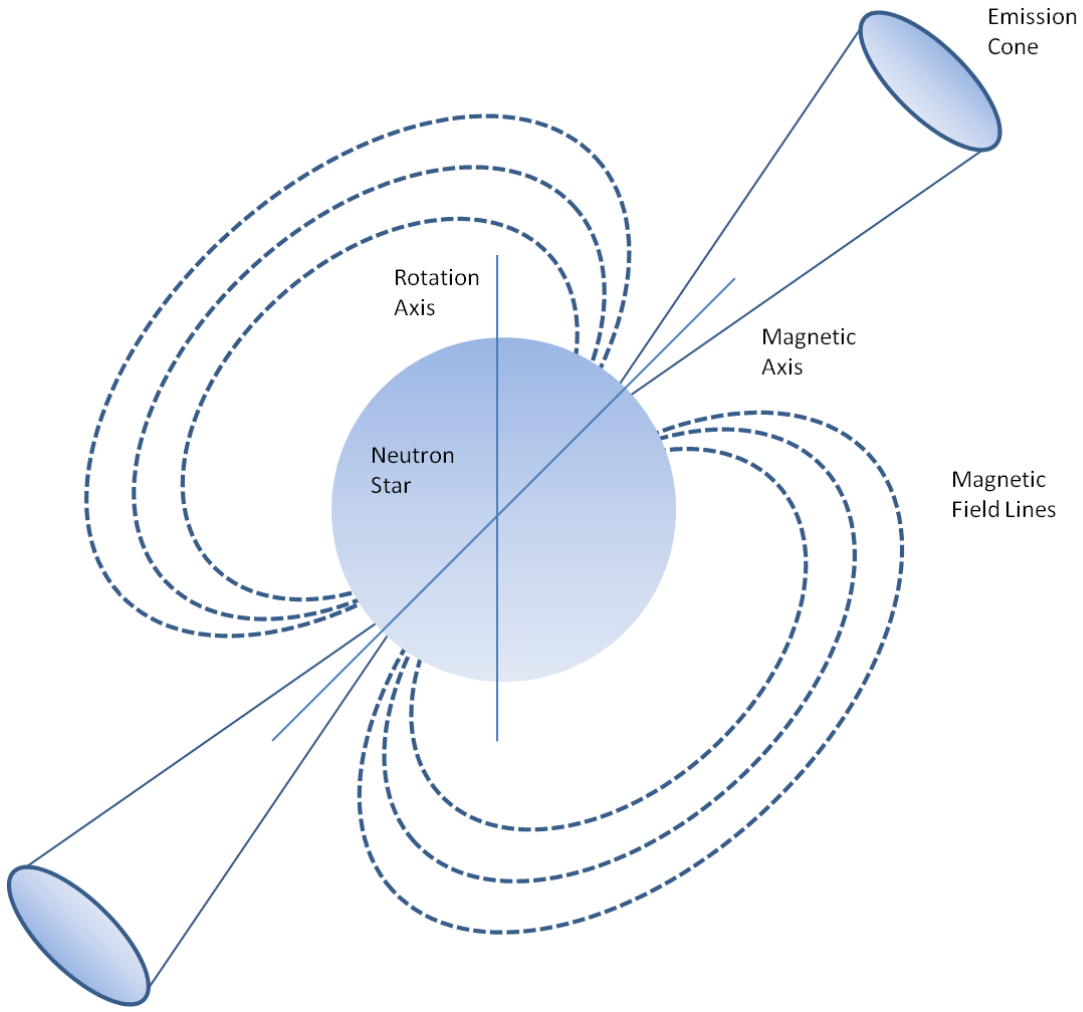

Figure 3: Not-to-scale drawing of a pulsar and its surroundings. Note the rotation axis and the magnetic axis are different. If the earth is on the line of site of the emission cone then we will see regular pulses.

It is generally accepted that a cone shaped beam centred on the magnetic axis of a pulsar accounts for many of the observations of a pulsar's pulse profile. The line of sight trajectory cuts the emission cone giving us a view of a curved slice of this beam (Lorimer & Kramer 2005, p67).

There are a number of different hypotheses regarding the actual structure of this beam. The two main competing models are the nested cone structure (Rankin 1993) and the patchy beam structure (Lyne & Manchester 1988).

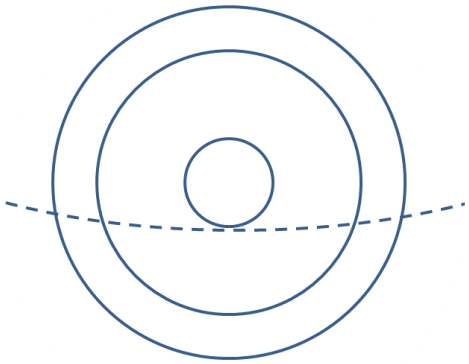

Figure 4: Nested cone structure of Rankin (1993). This is looking down the emission cone and the dotted line is the sight-line from Earth.

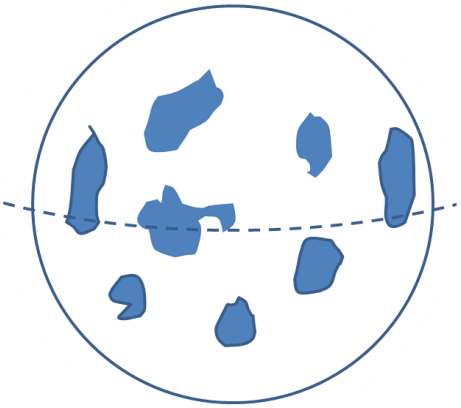

Figure 5: Patchy beam model of Lyne & Manchester (1988). Again, this is looking down the emission cone and the dotted line is the sight line from Earth.

These are used to explain the multiple peaks and micro-structure that occurs in the pulses.

An example is shown in Figure 6.

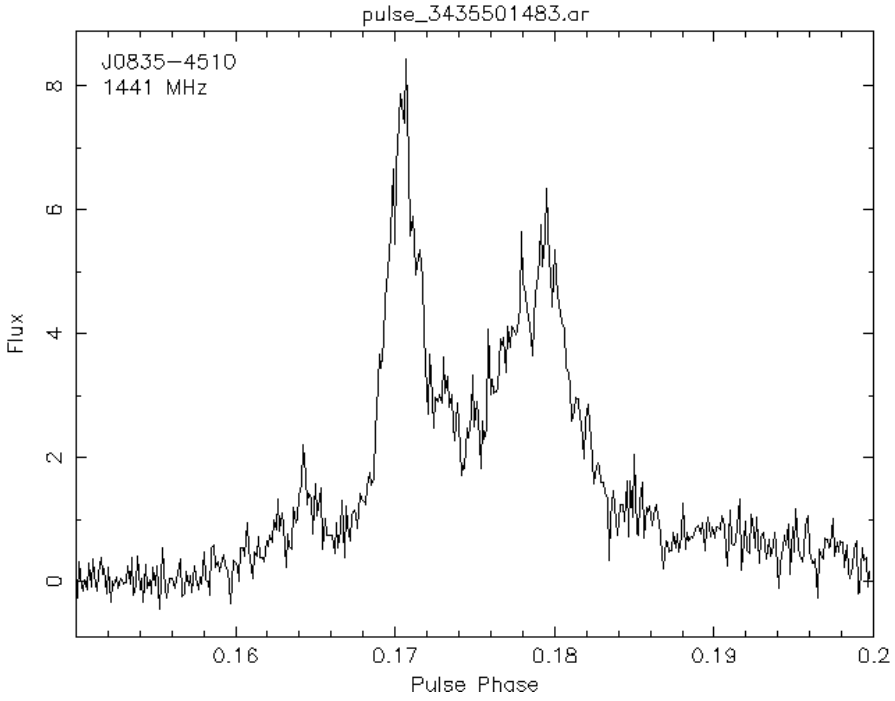

Figure 6: Micro structure and multiple peaks that can occur in a pulsar's pulse.

2.2. Frequency and Period

Due to the conservation of angular momentum, the neutron star can be spinning at a rapid rate. PSR B1937+21 was the fastest known at 642 Hz (Backer et al. 1982) which is a period of P=1.56 ms, but in 2006 PSR J1748-2446ad was discovered to be rotating at a frequency of 716 Hz which is P=1.40 ms (Hessels 2006).

The slowest known pulsar is J1841-0456 which has a period of 11.78 s (ATNF Pulsar Catalogue, Manchester et. al. 2005).

Figure 7 shows a histogram of log(period) of all known pulsars. It is very much bi-modal, however the bulk of the fast pulsars are binaries whereas the median of normal pulsars is around a period of 1 s.

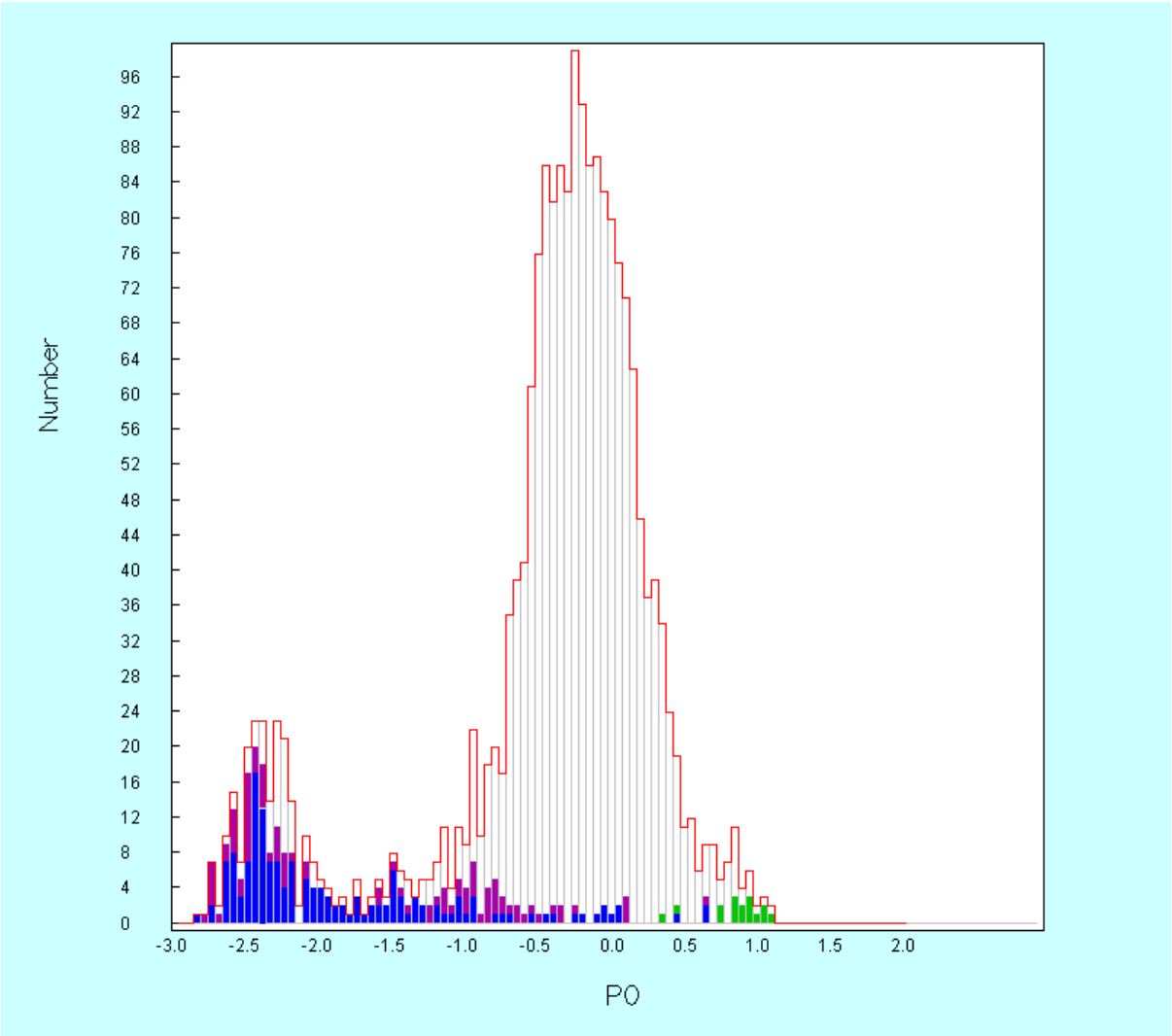

Figure 7: Histogram of log(period) of all known pulsars. Blue indicates binaries, green X-ray, and purple high energy pulsars (ATNF Pulsar Catalogue, Manchester et. al. 2005).

Pulsars slow down with time and so pulsar period's increase. Useful information can be derived from this. For example the spin down luminosity:

$$\dot{E} = 4\pi^2 I \dot{P} P^{-3}$$

(where $I = 10^{38}$ kg m^2 is the moment of inertia, P is the period and $\dot{P} = \frac{dP}{dt}$ is the period derivative) gives the total theoretical power output of the neutron star.

We can also derive the age of a pulsar from P and Ṗ:

$$T = \frac{P}{(n-1)\dot{\mathrm{P}}}\left[1 - \left(\frac{P_0}{P}\right)^{n-1}\right]$$

Where P_0 is the spin period when the neutron star was formed and *n* is the *braking index* which is the value of *n* for

$$v' = -Kv^n$$

where the frequency $v = 1/P$ and v'=*dv/dt*. The braking index for a pure magnetic dipole is *n = 3*, and actual braking indexes in real pulsars vary between 1.4 and 2.9 (Kaspi & Helfand 2002). However if P_0 is assumed to be small with respect to P and we set *n*=3 for simplicity, the *characteristic* age of the pulsar:

$$\tau = \frac{P}{2\dot{\mathrm{P}}}$$

is an approximation of the age of the pulsar. The assumptions regarding P_0 and *n* above are known to produce errors when comparing actual age with characteristic age of pulsars for which we know the date of formation (e.g. The Crab). Nevertheless we still tend to use characteristic age when comparing different pulsars.

Figure 8 shows a histogram of the log(characteristic age) of all known pulsars. The median is around 10^7 years of age.

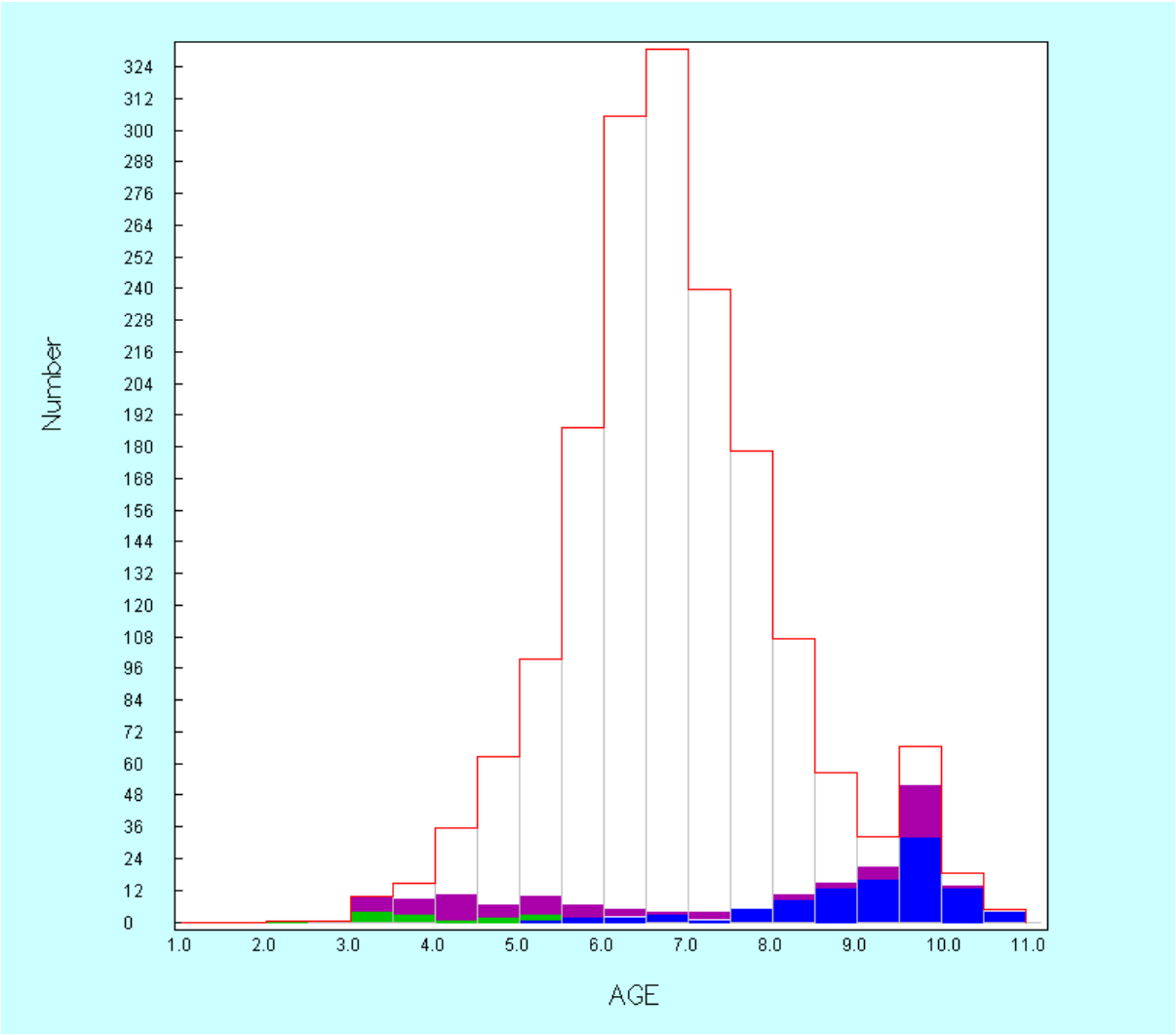

Figure 8: Histogram of log(characteristic age) of known pulsars. Colours are the same as in the previous figure. (ATNF Pulsar Catalogue, Manchester et. al. 2005).

2.3. Location of Pulsars Within the Galaxy

Figure 9 shows a plot of galactic latitude and longitude of all known pulsars. (Note that for ease of viewing, the longitude has been formatted as -180 to 180 instead of the normal 0 to 360). As can be seen they are fairly evenly distributed throughout the populous parts of the galaxy. Note the clusters of pulsars in the Large and Small Magellanic Clouds.

Note that the Vela pulsar is at galactic longitude -97 and latitude -3 on this map.

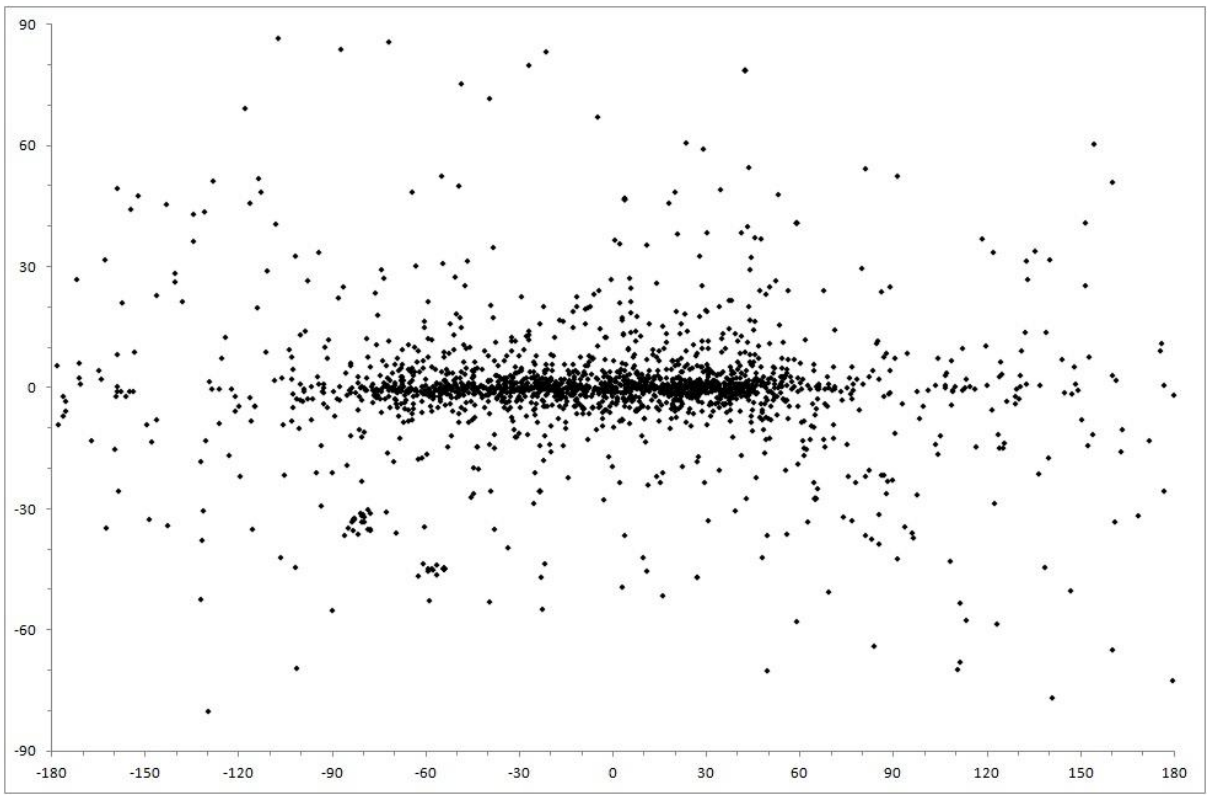

Figure 9: Plot of all known pulsars by galactic latitude v longitude (represented as -180 to 180). (Data from ATNF Pulsar Catalogue, Manchester et. al. 2005).

2.4. Light Cylinder and Polar Cap

The plasma surrounding the neutron star rigidly co-rotates with the star itself (Lorimer & Kramer, 2005). However once the co-rotating plasma reaches a certain distance from the pulsar it would need to be travelling at the speed of light. This distance is:

$$R_{LC} = \frac{cP}{2\pi}$$

where c = 299,792,458 ms^{-1} is the speed of light. Magnetic field lines within this light cylinder are closed and the ones outside remain open. These mark the boundary of the emitting polar cap. The radius of this polar cap can be approximated by:

$$R_p = \sqrt{\frac{2\pi R^3}{cP}}$$

For Vela, and B0943+10 (the subject of Deshpande and Rankin's 1999 paper – see Chapter 3) some of the key figures just discussed are shown in Table 1.

Measure	Symbol	Vela	B0943+10	Unit
Period	P	89.328385024 x 10^{-3}	1.09770570486	s
Period derivative	Ṗ	1.25008 x 10^{-13}	3.49339 x 10^{-15}	ss^{-1}
Spin down luminosity	Ė	6.9 x 10^{36}	1 x 10^{32}	ergs s^{-1}
Characteristic age	τ	1130	4.98 x 10^{6}	years
Light cylinder radius	R_{LC}	4262.166	52375.328	km
Polar cap radius	R_p	484	138	m

Table 1: Key parameters for the Vela pulsar (J0835-4510) and B0943+10 (ATNF Pulsar Catalogue, Manchester et. al. 2005).

2.5. Interstellar Medium

Space between the pulsar and the observer is not empty. It in fact contains cold ionised plasma (Lorimer & Kramer p85). Electromagnetic radiation from pulsars is affected by the

interstellar medium (ISM) in a number of ways. Most notable are frequency dispersion and scintillation.

Dispersion is where lower frequencies arrive later than higher frequencies. The difference in arrival time can be approximated by:

$$\Delta t = 4.15 \times 10^6 \left(\frac{1}{f_1^2} - \frac{1}{f_2^2} \right) \int_0^d n_e \, dl \ \text{(ms)}$$

Where the frequencies are in MHz and

$$DM = \int_0^d n_e \, dl$$

is a constant for each pulsar known as the Dispersion Measure, and is the integral of the electron column density between the observer and the pulsar. For Vela,
the DM = 67.99 cm^{-3} pc and so the time delay between frequency channels is:

$$\Delta t = 282.1585 \times 10^6 \left(\frac{1}{f_1^2} - \frac{1}{f_2^2} \right) \text{(ms)}$$

Note that the DM can be derived from observation and if the electron density is known (e.g. from Cordes & Lazio, 2002), then the distance to the pulsar can be calculated. If the pulsar distance is already known from other methods, then a more accurate electron density can be calculated.

The ISM also causes scintillation – i.e. changes in intensity similar to our atmosphere causing the stars to twinkle. Since this thesis is discussing observations of bright vs normal pulses, scintillation is an important topic to cover.

The ISM is turbulent and “lumpy” - this was discovered as affecting pulsars by Lyne and Ricket (1968). Soon after, Scheuer (1968) developed a proper scintillation theory by modelling the ISM as a single thin screen halfway between the pulsar and Earth.

This screen causes a diffraction pattern to appear as the Earth moves through the solar system, and this causes apparent changes in the flux density of the pulsar. The nature of these changes is dependent on the scintillation time scale and the scintillation bandwidth. The time scale gives an indication of over what time frame changes in flux density will be observed. The scintillation bandwidth gives an indication of whether these changes can be observed with the equipment. If the scintillation bandwidth is larger than the observation bandwidth, scintillation will not be observed.

We know from Cordes & Lazio (2002) that in the direction of J0835-4510, the scintillation bandwidth is 30 kHz (much smaller than our observation bandwidth, so we should be able to detect it). But more importantly the time scale is approximately 30 s.

As will be discussed later in Chapter 5.2, it turns out that scintillation has no effect on our consecutive bright pulse observations.

2.6. Glitches

Some pulsars (including Vela) are known to occasionally show a brief increase in rotation, colloquially known as “glitches” (Dodson et al, 2007). Typically the increase in rotation occurs and then it relaxes back to its previous level over a period of months.

These are an intriguing property and various explanations as to why these glitches occur have been put forward over the years. Michel (1970) proposed that a planet in an elliptical orbit could produce glitches in Vela. However the irregularity of these glitches as shown by Dodson et al (2007) seems to rule this out.

A more robust explanation is that the crust of the pulsar rotates around a super-fluid core, and that these sometimes detach from each other causing the pulsar to briefly speed up and then slowly restore to equilibrium over time. (Link et al, 1992)

Another more recent explanation is the effect of tiny vortices within the internal super-fluid. (Pizzochero, 2011).

Glitches remain an intriguing phenomenon and are a fruitful area of pulsar research.

2.7. Definitions

A strict naming convention for different single pulse flux densities has not been formalised in the literature. Giant pulses are typically defined as being at least 10 times the flux density of the average pulse integrated over the entire pulse window (Johnston et al. 2001). A "giant micro pulse" (Johnston et al. 2001) is a pulse that has a high peak flux density and typically has a FWHM of under 500 μs. A "sub-pulse" is a single pulse that is narrower than the mean pulse envelope. A "drifting sub-pulse" is a sequence of sub-pulses which drift monotonically in longitude with each successive pulse (Edwards and Stappers 2008).

We define a "consecutive sub-pulse" to be a sub-pulse that occurs from one rotation to the next but does not appear as a permanent feature in the mean pulse profile. We also define

a “bright” pulse as one that is at least five times the flux density of the average pulse integrated over the entire pulse window; half the threshold for a true giant pulse but significantly greater than the average. Consequently, a “bright sub-pulse” is one that is both bright and a sub-pulse. The term “bright pulse” also will mean a “bright sub pulse”.

2.8. Giant Pulses in the Crab Pulsar

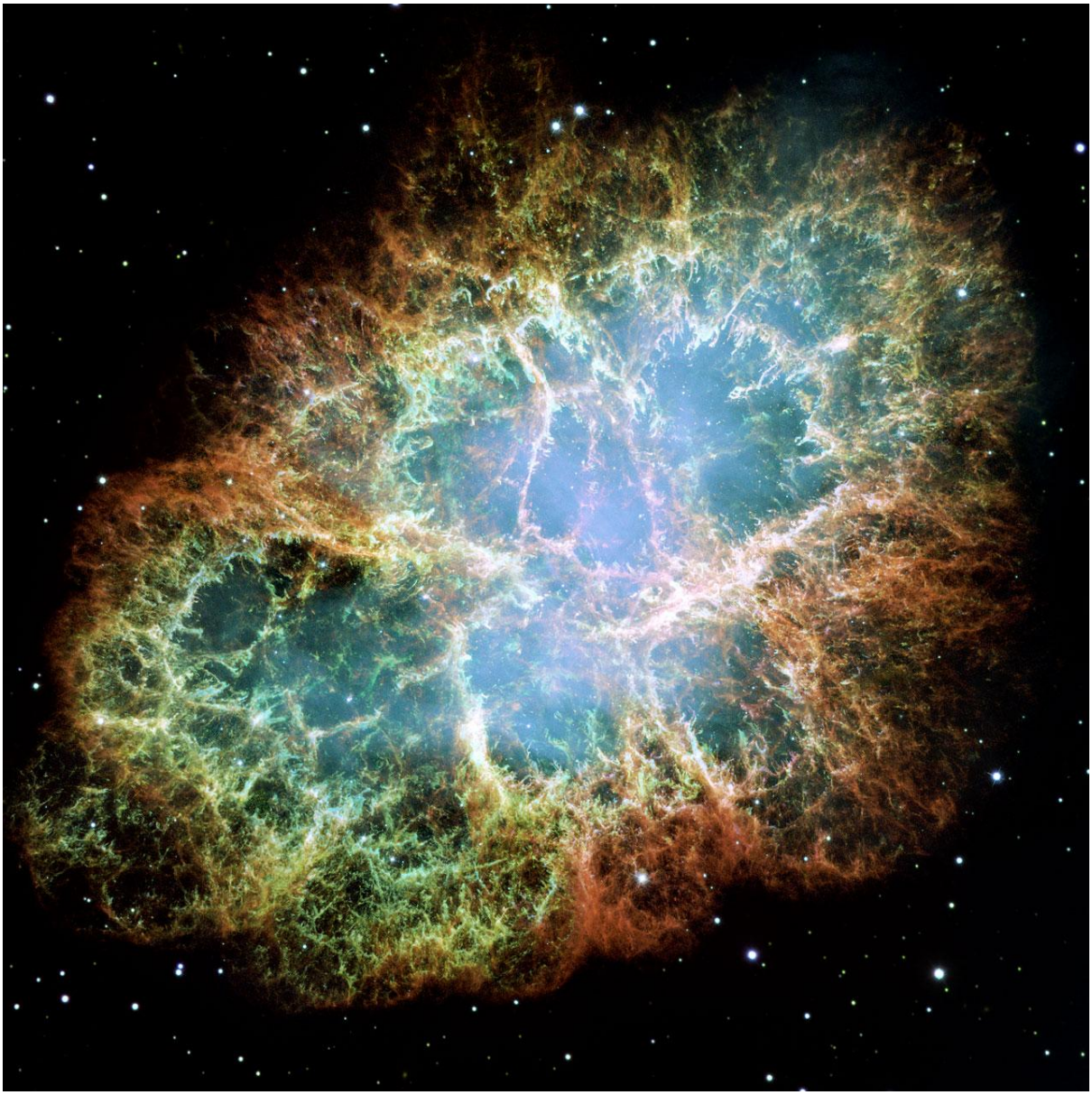

Figure 10: The Crab supernova remnant from the Hubble Space Telescope. (NASA, ESA and Allison Loll/Jeff Hester (Arizona State University). Acknowledgement: Davide De Martin (ESA/Hubble).

Supernova SN 1054 left behind the Crab nebula and within it sits the Crab pulsar (PSR B0531+21) which is the second brightest pulsar in the northern sky (Karuppusamy et al. 2010). The Crab pulsar has the magnetic axis nearly perpendicular to the rotational axis and

so we see two pulses (a main pulse and an interpulse) as each emission cone passes over the earth.

The Crab pulsar is one of a small number of pulsars that emits true giant pulses and Hankins & Eilek (2007) showed that these giant pulses can be as narrow as 0.4 ns. It has also been shown that narrower pulses tend to be brighter (Popov & Stappers 2007).

Karuppusamy et al. (2010) found that the Crab also occasionally emits "double giant pulses" – i.e. a giant pulse on the main pulse and another, straight after, on the interpulse. Studies of these "doubles" showed they were independent chance events, as one would expect, given they were emitted from opposite ends of the neutron star.

Karuppusamy et al. (2010) says in the discussion:

> *"From the measured pulse widths and the observed structure in many pulses, it is evident from the analysis presented in this paper that the giant pulse emission is a manifestation of temporal plasma changes in the pulsar magnetosphere. The observed giant pulse rates are further evidence for this temporal variation, because if the mechanism responsible for the giant pulses is active on timescales longer than a pulse period, a clear excess of giant pulses separated by a single rotation period can be expected."*

followed by:

> *"On the basis of the giant pulse arrival times, it was concluded that the observed giant pulse emission does not come from a steady emission beam loosely bound to the stellar surface"*

As we will show in Chapter 5, Vela does emit such consecutive bright pulses and we agree that these are due to temporal changes of the plasma in the pulsar magnetosphere.

2.9. Vela Supernova Remnant and PSR J0835-4510

The Vela Supernova Remnant lies at a distance of 290 pc (~ 950 ly) in the southern constellation of Vela and is approximately 32 pc across (7.3° in the sky). The original supernova exploded around 11400 years ago (Cha et al., 1999) and within lies the Vela pulsar (PSR J0835-4510).

Optically the Vela pulsar is very faint (V = 23.6), however it is still the third brightest of all isolated neutron stars (Mignani et al., 2007). Visually the period of its pulses match the radio pulses (Wallace et al., 1977) and studies at many optical wavelengths all point to a non-thermal magnetospheric origin of the radiation (Mignani et al., 2007).

Mignani (2007) also shows that at optical wavelengths, its visual flux density (F_v) follows a fairly flat power-law distribution between 4000 and 8000 Å with:

$$F_v \propto \nu^{-\alpha}$$

where v is frequency and $\alpha = -0.04 \pm 0.04$.

3.Emission Mechanisms and Bright Pulses

3.1. Emission

The pulsar emission process is still relatively unknown. Of all known pulsars, radio emission occurs from around 100 MHz to 100 GHz (Lorimer & Kramer p82) and high energy emission occurs in X-rays and gamma rays. Wrapping all this into a single model is still one of the large unanswered questions in pulsar astronomy.

Needless to say a number of radio emission models have been proposed and refined (and some discarded) over the years. Most of these models place the emission in the magnetosphere and tend to be focused on the average radio pulse rather than bright or giant pulses.

The literature seems to generally consider the average pulse as “normal” and views the bright or giant pulses as the exception.

For example Karastergiou & Johnston (2007) attempt to reconcile the nested cone models (Rankin, 1983) and the patchy beam model (Lyne & Manchester, 1988) with the empirical evidence.

They propose an empirical model of radio pulsar beams that is based on the idea that radio emission of certain frequencies occurs at different heights in the pulsar magnetosphere. According to their model, pulsars have different emission layers (called “heights” in the paper) and each layer can have one or more emission patches. Younger pulsars have a smaller number of emission heights with a small number of emission patches per height. Older slower pulsars have more emission heights and more emission patches per height.

This accounts for the observation that typically older pulsars have more complex pulse profiles.

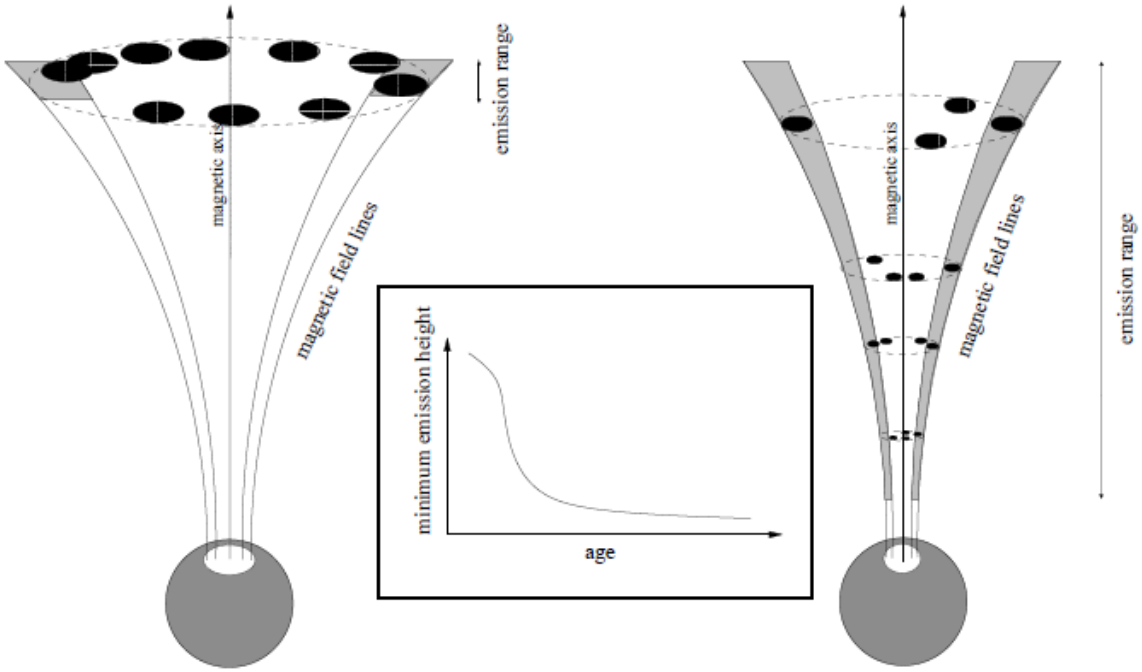

Figure 11: Diagram from Karastergiou & Johnston (2007) showing proposed emission layers and patches within those layers for young pulsars on the left and old pulsars on the right.

Their model has six “ingredients” (reproduced from the paper):

1. Radio emission originates from field lines close to the outer edge of the beam, forming an emission cone.
2. The conal beam is patchy.
3. The maximum altitude of emission, in all pulsars, is set to ~1000 km at a frequency of ~1 GHz.
4. The minimum altitude of emission is large for young pulsars (similar to the maximum altitude) and small (~20 km) for older pulsars.

5. Emission arising from discrete locations within the entire range of emission heights is possible at a given frequency.
6. The polarisation position angle of each patch is tied to the magnetic field line at the centre of that patch.

Their definition of “old” vs “new” is defined as P > 150 ms and P < 150 ms respectively and is based on the observation of 250 pulsar profiles. The interesting fact that the profiles of pulsars with P < 150 ms have 60% single components and 40% double components, whereas with P >150 ms there is 45% with single, 25% with double and 30% with multiple components. So Karastergiou & Johnston have elected to split their model into two, based on this evidence.

This model has taken a view of a large number of different types of pulsars and attempted to generate an empirical model. Unfortunately this model does not contemplate bright or giant pulses. So the possible reasons why one or more of these emission patches suddenly goes bright is not covered. A hypothesis here could be a lining up of patches on different layers. However since Vela (P = 89.3 ms) is a young pulsar it would, according to their model, only have a single layer.

However Johnston et al. (2001) studied 20,085 single pulses (approximately 30 minutes worth) of the Vela pulsar at 660 and 1413 MHz on 2000 March 14-17. At the higher frequency the time resolution was 44 μs and is notable for being the first publication of observations of microstructure in the Vela pulsar. The paper reports that 95% of the pulse amplitudes are within a factor of 2 of the mean flux density and 99.5% are within a factor of 3, and that there are no pulses greater than 10 times the mean flux density.

Of note in this paper is the discovery of giant micro pulses. These are pulses that have a large peak flux density, but are very narrow. The paper notes the brightest pulse as one which is 40 times the peak flux density of the mean pulse but with a FWHM of ~50 μs. (See Chapter 6 for further discussion of this.)

A key point is that these giant micro pulses arrived at an early phase in the pulse profile. On average about 1.5 ms, and the earliest up to 2 ms, prior to the peak of the mean pulse profile.

3.2. Drifting Sub-pulses

Some pulsars exhibit drifting sub-pulses and Deshpande & Rankin (1999) analysed the drifting sub-pulses in B0943+10 and showed that they are caused by a rotating frame of emission centres circulating around the magnetic pole.

Figure 12 shows the drifting sub-pulses as observed over time.

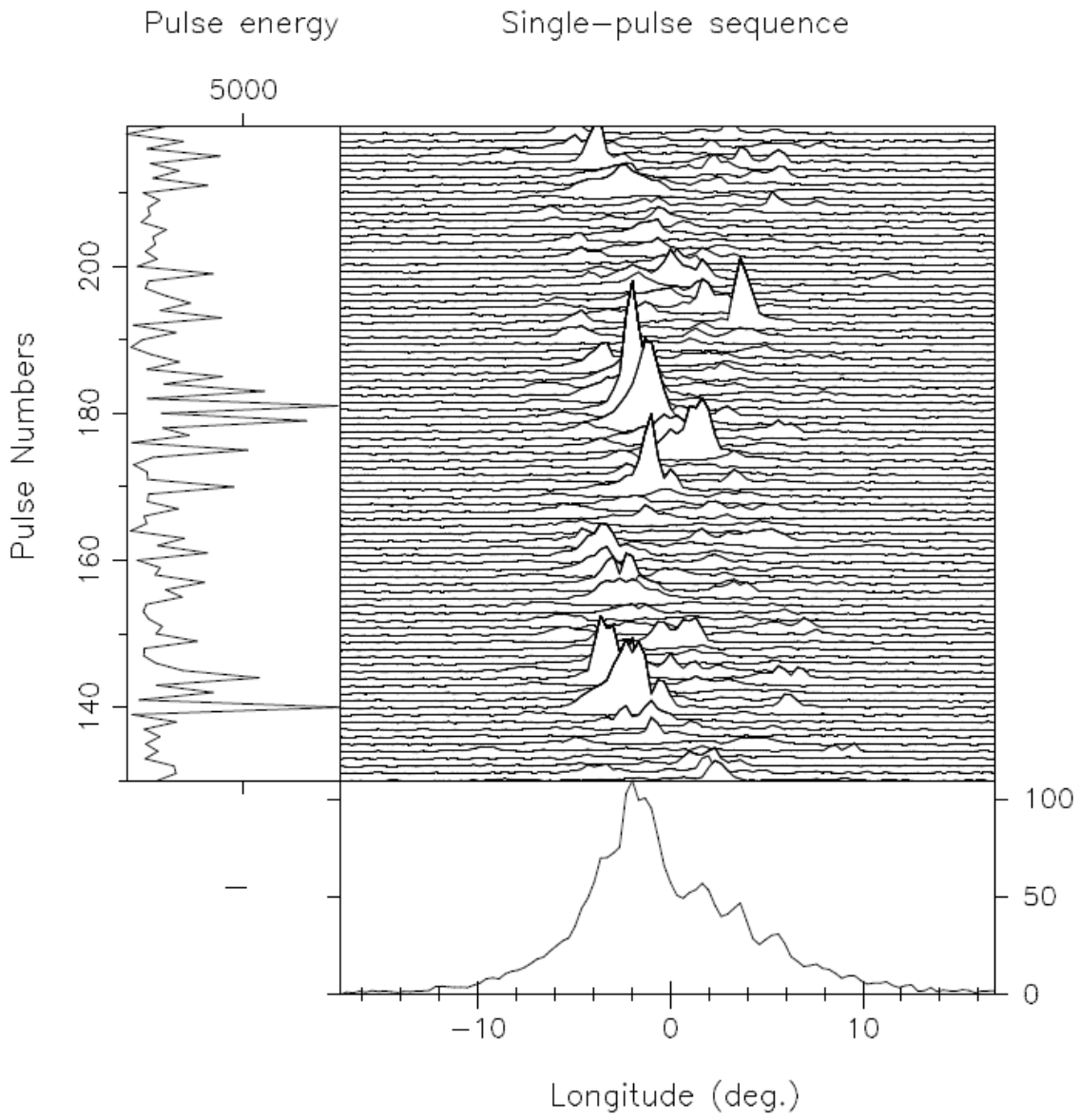

Figure 12: Drifting sub pulses from B0943+10 from Deshpande & Rankin (1999)

They Fourier transformed the entire pulse sequence and found 20 emission centres that rotate about the magnetic pole every 37.35±0.02 periods (or about 41 seconds). Note the sight-line traverse in Figure 13 which shows the sampling that occurs as these emission centres slowly rotate about the magnetic pole.

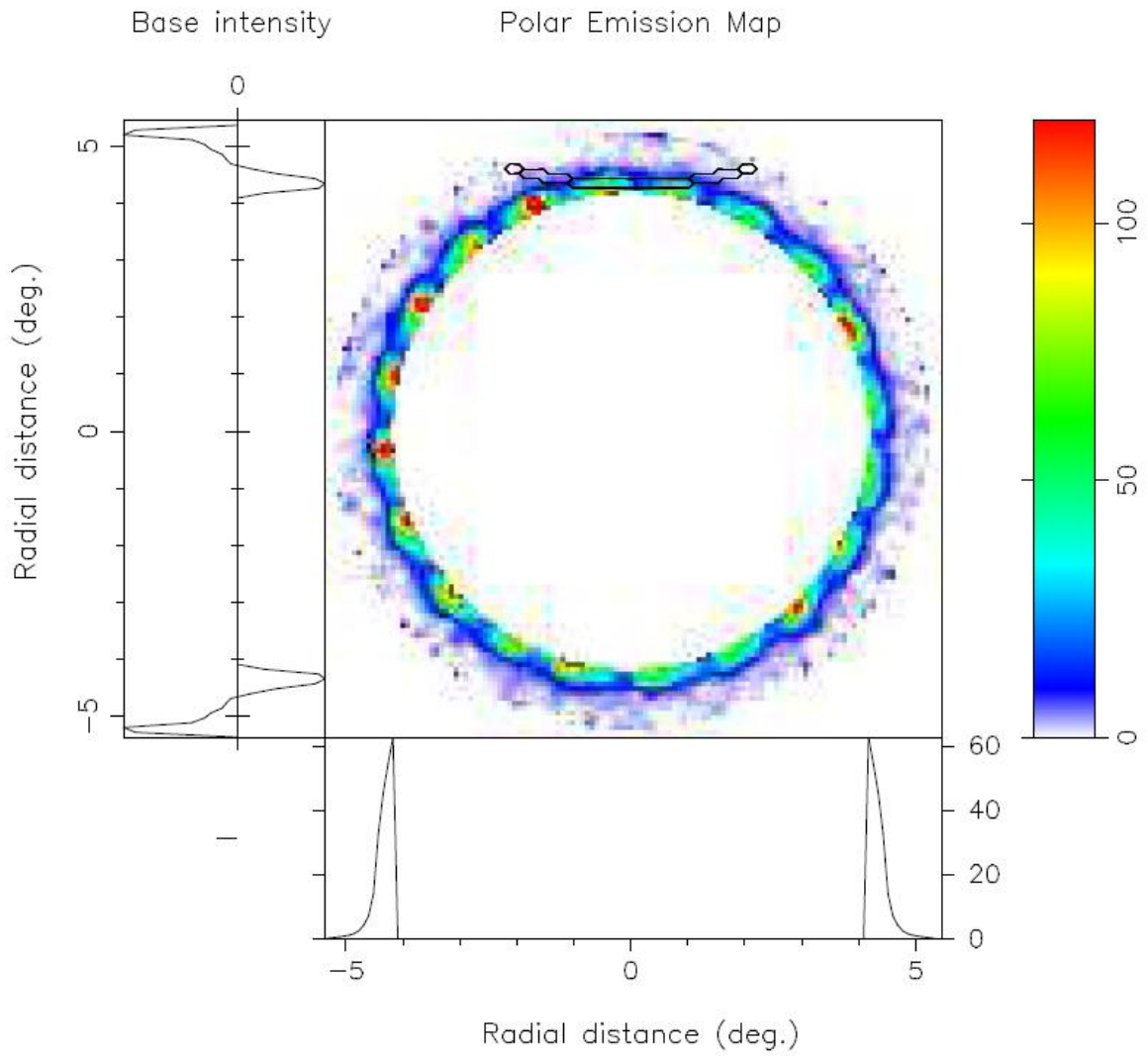

Figure 13: Rotating carousel of emission centres from Deshpande & Rankin (1999)

Deshpande and Rankin note that these emission centres are not entirely stable in that they sometimes bifurcate and rejoin, as well as varying in intensity and azimuthal spacing. However over time these 20 emission centres are remarkably stable.

The observation frequency is also critical here. They calculated a similar map at 111.5 MHz, where the sightline traverses interior to the 430 MHz one, and that “shows a more nearly circular sub-beam shape”.

Although B0943+10 is quite different from Vela (which doesn't have drifting sub pulses) in that its rotation period is 1.098 s (as compared to 89.3 ms) it also doesn't emit at high frequencies. The observations for this paper were at 430 MHz.

However the results perhaps can provide insight into the nature of the consecutive bright pulses found (see Chapter 5) on Vela because it is possible that there exists a rotating carousel as well, which occasionally is cut by the line of sight trajectory.

3.3. A Different Approach

Kontorovich (2009) contemplates a different approach to the pulsar beam model. Colloquially put, he proposes that the giant pulse is a view of the emission near the surface through a gap in the magnetosphere, and the regular pulse is a view of the emission masked out by the magnetosphere. Figure 14 is a not-to-scale representation of this.

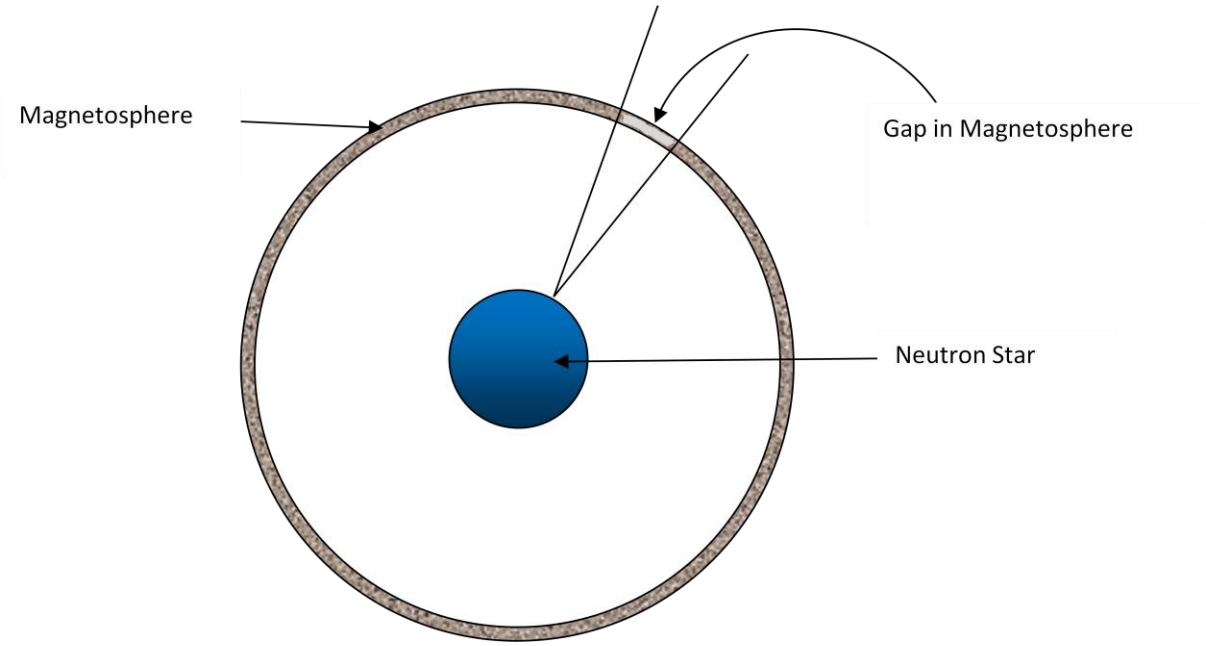

Figure 14: Not-to-scale picture showing neutron star, magnetosphere, and gap. See text.

The emission near the surface is caused by: "*...the internal vacuum gap is a cavity resonator stimulated by discharges and radiating through the breaks in the magnetosphere*".

So rather than the normal pulse being the standard emission from the magnetosphere and the bright pulse being explained by some "extra" emission, Kontorovich says the bright pulse is a clear view of the emission (near the surface of the neutron star) through a gap in the magnetosphere, and that the normal pulse is viewing the emission being blocked by the magnetosphere.

Kontorovich also notes that the bright pulses line up with the hard pulsar emissions of X-rays and gamma-rays.

---

4. Instrumentation, Software, and Data Collection

4.1. Mount Pleasant

Figure 15: The 26 m radio telescope at Mt Pleasant near Hobart, Tasmania. (Photograph by Jim Palfreyman)

Observations were mostly made with the University of Tasmania's 26 m radio telescope based at Mt Pleasant, near Hobart, Australia. The centre frequency of these observations was mainly at 1440 MHz with bandwidth 64 MHz. (Although other frequencies were used as well, the bulk of the data was collected at 1440 MHz.)

The receiver consists of a cooled 20 cm prime-focus feed-horn with dual linear polarisation feeds that were sampled by an analogue to digital converter using 2 bit precision at 128

million samples per second that were recorded directly onto a Redundant Array of Independent Disks.

Collection processing was done using the software packages DSPSR (van Straten & Bailes 2011).

DSPSR is an open-source high performance digital signal processing software package which performs, amongst other things, phase-coherent de-dispersion and automatic excision of invalid data.

As explained in Section 2.5, electromagnetic waves propagating through the interstellar medium arrive at different times depending on frequency. DSPSR corrects these delays in each frequency channel.

At Mt Pleasant we had 16 frequency channels and 8192 pulse phase bins over the 89.3 ms pulse period. This gave a time resolution of 10.9 µs.

Polarisation data was stored in each data file, although it was not closely analysed for this thesis.

Each raw data file contains 10 seconds (or 112 pulses) worth of data. Each 10 second file is 640 Mb in size and so they are processed - drastically reducing their size - and then the processed files are archived. The raw files were then deleted to conserve space.

4.2. Parkes

Figure 16: The 64 m telescope at Parkes, NSW. (Photograph by Jim Palfreyman)

A fortuitous collection of single pulse data occurred during an unallocated session of "Director's time" at the Parkes 64 m radio telescope which was courtesy of Willem van Straten. It was only an hour of data on 2009-1-07 that generated 43000 pulses. Unfortunately, due to the short notice and scheduling conflicts, we couldn't get a simultaneous observation at Mt Pleasant – which would have been ideal.

This data was collected from the central beam of the 21cm multi-beam receiver with the Swinburne APSR instrument.

DSPSR was also used for processing, but unlike Mt Pleasant which observes at a single frequency, there were 16 separate sub-bands (1249, 1265, 1281, 1297, 1313, 1329, 1345,

1361, 1377, 1393, 1409, 1425, 1441, 1457, 1473, and 1489 MHz) recorded simultaneously each with 32 frequency channels of 16 MHz bandwidth. As with Mt Pleasant there were 8192 phase bins, but each data file contains a single pulse of 89.3 ms in duration again with 10.9 μs resolution.

4.3. Analysis

General analysis of the processed data was done using PSRCHIVE (Hotan, van Straten & Manchester 2004). This open-source software provides a suite of pulsar analysis tools including: data file manipulation, plotting, polarisation, arrival times, dispersion measure calculations, single pulse analysis, and much more.

The suite, at the time, came with a program for single pulse analysis called “spa”. This program essentially scanned through the pulsar files, determining the average flux density and then looked for pulses at a cut-off factor a certain number of times greater than that average flux density level. This cut-off level did vary slightly from observation to observation (most likely due to scintillation and perhaps height of the pulsar above the horizon).

We modified the spa program to also produce a table of bright pulses that included the peak flux density level and the width of the bright pulse. The width (or FWHM – Full Width at Half Maximum) was calculated by searching out the peak value for the pulse, moved down to half that value and then searching out sideways for the pulse. That width was then marked as the pulse width. See Figure 17. Note that for multiple peaks like in Figure 29, only the highest one would be measured. Whilst this could be considered a weakness, this algorithm is highly sensitive to tall narrow pulses – which we were looking for.

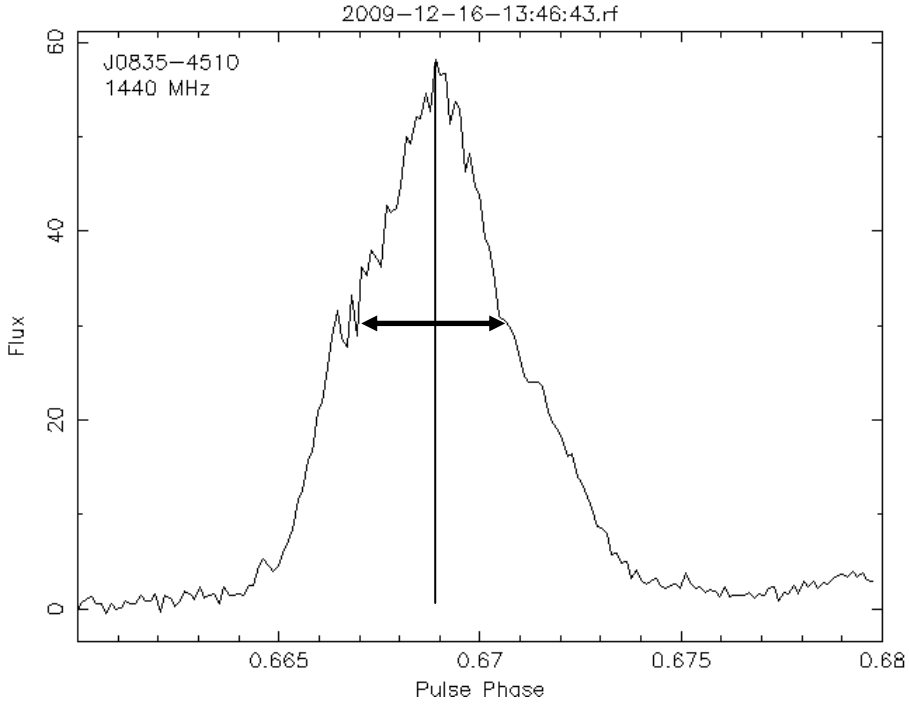

Figure 17: Explanation of how Full Width Half Maximum (FWHM) is calculated. For multiple peaks, obviously only the highest peak will be measured.

4.4. Interference

Interference is a constant problem for the Mt Pleasant radio telescope. Hobart Airport is approximately 7 km southeast, and Hobart city (as well as some nearby transmitters) are in the southwest direction. Even though Vela is circumpolar in Hobart, interference was a potential issue when the pulsar was low in the sky.

When averaging many pulses, occasional interference is not a problem. However, when searching for bright pulses our software would potentially report interference as a bright pulse – or even more likely a consecutive bright pulse.

So once the bright pulses were identified, a sorted list of consecutive bright pulses was created. From the top of the list down, each and every data file that supposedly contained

two or more consecutive bright pulses was manually examined. If it was found to have interference it was discarded.

Even though this sounds a long and tedious process, it turned out to be fairly straightforward and not too time consuming. By starting at the top of the sorted list, many of the bad data files were eliminated quickly. This caused a cascading effect as false positive sections throughout the list were removed.

New transmitters are also an issue in the region of Hobart, and due to a lack of communication from the ATNF to the University of Tasmania; a nearby police transmitter was set into permanent operation in late 2010, completely destroying future observations at 1440 MHz.

4.5. Data Collected and Archiving

The overall data collection plan was aimed at about 4 hours observation each weekend for a number of years. Whilst the full collection plan didn't eventuate due to a number of factors (e.g. scheduling conflicts, high winds, and hardware issues), a significant amount of data was collected and processed.

Actual processing of collected raw data over the years was performed on a number of different computers. The early machines would take about three days to process a 4 h observation run. However, about half way through the project the installation of six new computers, each with 8 CPUs, and a connection through to the Tasmania Partnership of Advanced Computing's (TPAC) data store was completed. Processing and archiving of data then became nearly real-time. Even though we had this near real-time processing capability,

we didn't use this very often since as long as the data was processed in time for the next observation, all was ok.

The TPAC data store has all files available for analysis, but with some being archived to tape automatically when regular usage has dropped off. Accessing the archived file triggers a restore from tape which can take a few minutes. This caused delays in processing but at least all processed data from this project has been retained.

4.6. The Software Fault

A major setback occurred when it was discovered halfway through the observing program that there was an introduced bug in the DSPSR processing software and that approximately a year's worth of processed data had been de-dispersed incorrectly. Since the original raw data files were not kept, it was impossible to restore the data, and a subsequent analysis found there was no way to correct the error. The data had to be discarded. (The data hasn't, at this writing, been actually erased – just set aside.)

We also collected data from the Ceduna radio telescope in tandem with Mt Pleasant, but at different frequencies. Unfortunately it was made useless by this software error as well.

To compensate for this setback and loss of data, an intense two week program of observation was commenced where Vela was observed at Mt Pleasant for 10 hours a day for ten days. This data set provided over 100 hours of data with no instrumentation changes between breaks in observation (these breaks were due to Vela being too close to the horizon for the telescope to observe).

This program made up for the loss of observations due to the software fault and provided some excellent results.

4.7. The Glitch

During the planned four year observing run it was hoped that Vela would glitch. Fortunately this occurred on 2010 July 31.802 UT, towards the end of planned observations, but still with enough time to gather an adequate amount of data.

This proved fortunate as the post-glitch data provided some very interesting results. (See Chapter 7.)

5.Bright Pulses in PSR J0835-4510

5.1. Bright or Giant pulses?

Vela has been stated to emit “bright” pulses, but not “giant” pulses (Johnston et al., 2001). This may be incorrect. True giant pulses appear to be rare – but they seem to have occurred. Whether these are true giants, however, is not the focus of this thesis, but a topic for further study.

Figure 18 and Figure 19 are the average pulse profiles of the Vela pulsar as observed from 6000 pulses from Mt Pleasant and 1000 pulses from Parkes. Note that even with 6 times the pulses, Mt Pleasant still has more noticeable noise.

Even so, the pulse profile is very clear – and they match as expected. The key point here is the height of this average pulse: roughly 1.2 and 4 for Mt Pleasant and Parkes respectively. This figure is the baseline for relative pulse heights throughout this study.

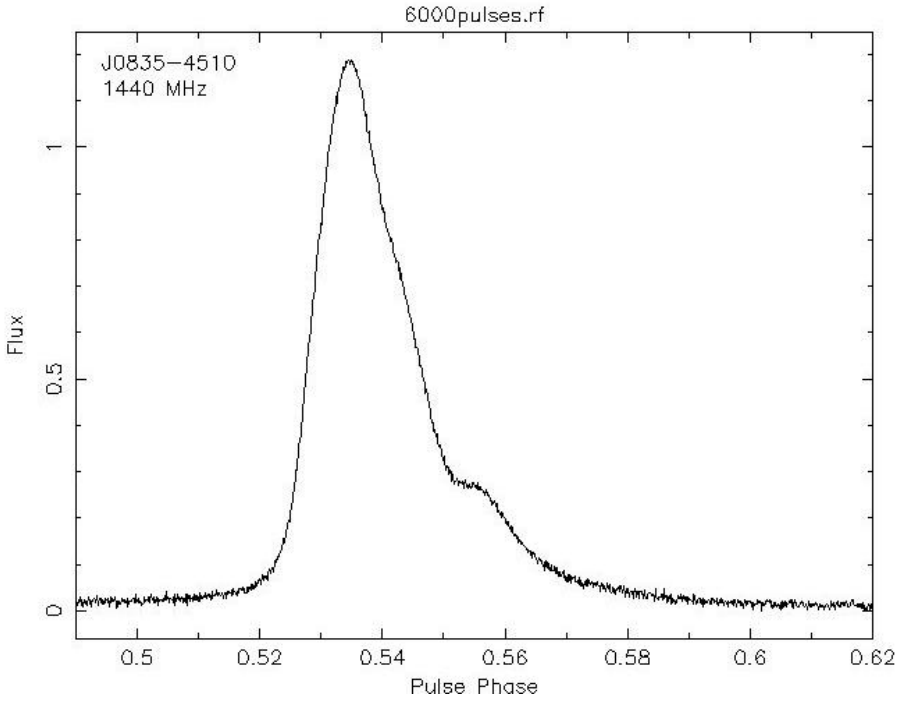

Figure 18: Mean pulse for Vela as observed at Mt Pleasant. This is the average of 6000 pulses.

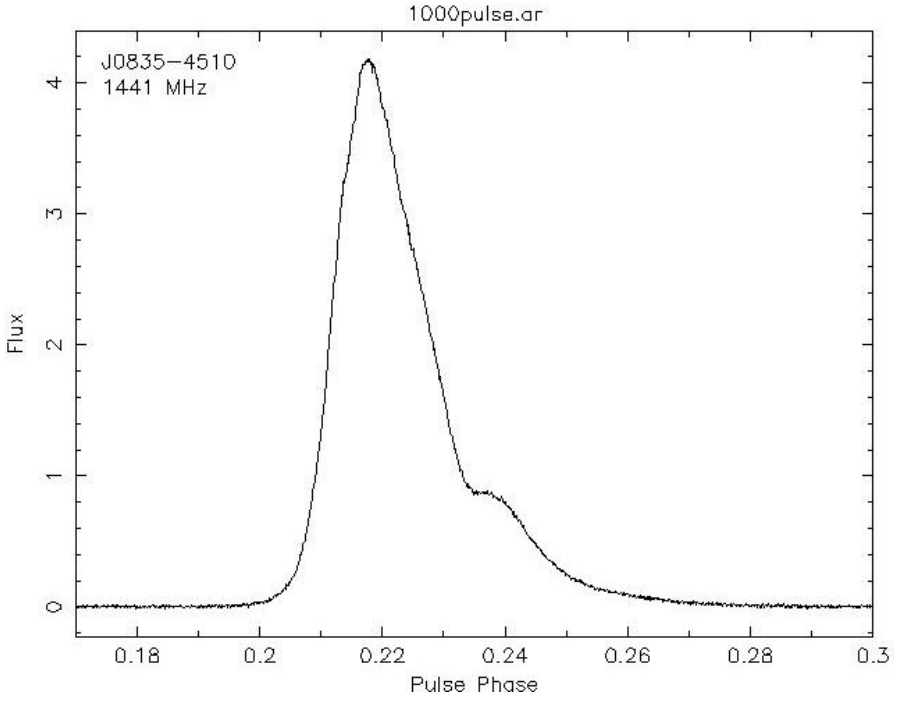

Figure 19: Mean pulse for Vela as observed at Parkes. This is the average of 1000 pulses.

When examined in detail, the brightest pulse in the Mt Pleasant data set peaked up around 60 times the normal regular pulse. From the general plot in Figure 20, and the magnified view in Figure 21, we can see there is some interesting activity in the pulses before and after the main bright pulse.

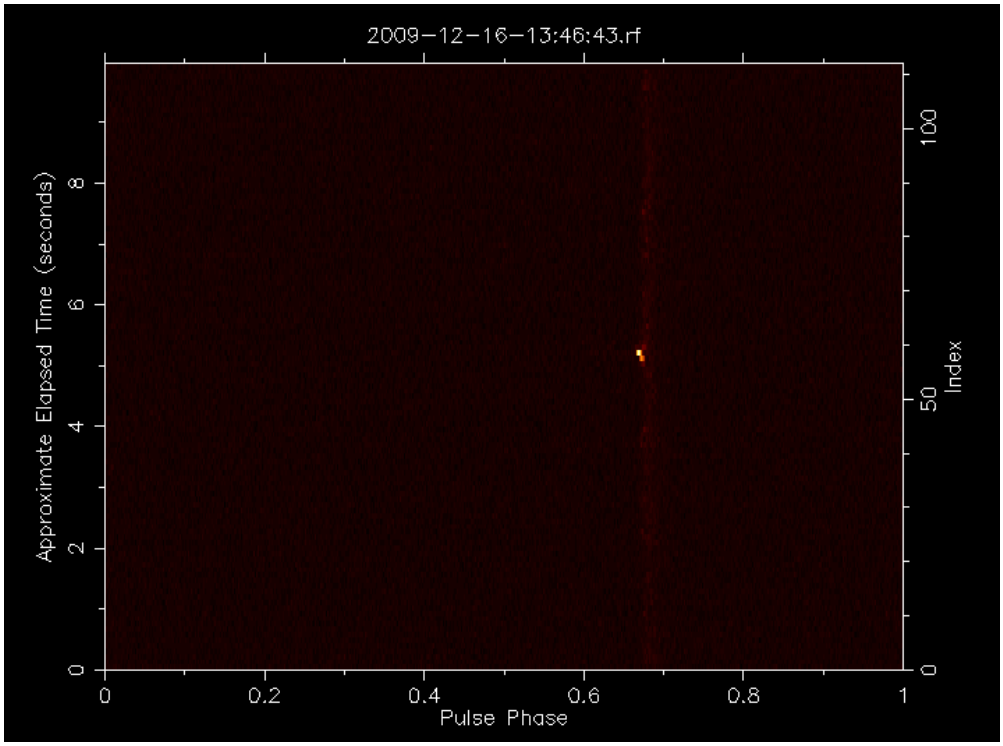

Figure 20: The brightest pulse in our observing runs at Mt Pleasant. This is 10 seconds, or 112 pulses, shown as a time vs time graph, folded at the period of the pulsar, which is represented as a phase from 0 to 1. The general pulses can be seen as a hazy line rising up the chart - just before a phase of 0.7. The bright pulse can be seen a bit after 5 elapsed seconds.

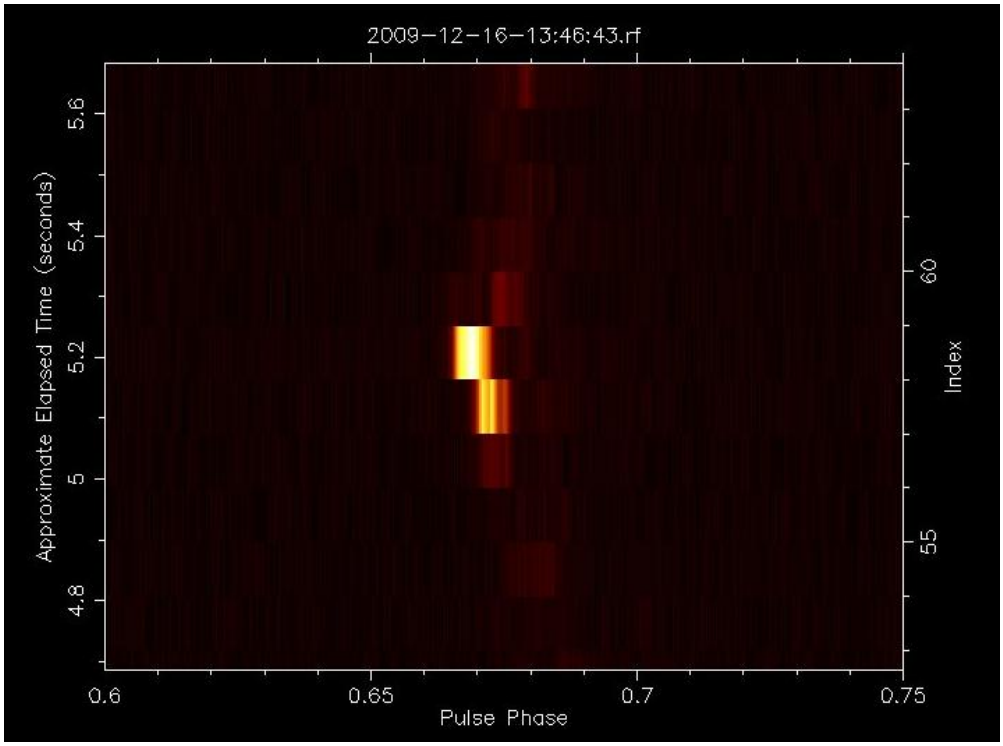

Figure 21: Magnified view of bright pulse in previous figure.

Shown in Figure 22 to Figure 25 is the microstructure detail of the two pulses prior to the bright pulse, the bright pulse itself, and the one after. Note that the y scale changes so we can see the microstructure in each pulse, but the time axis is identical.

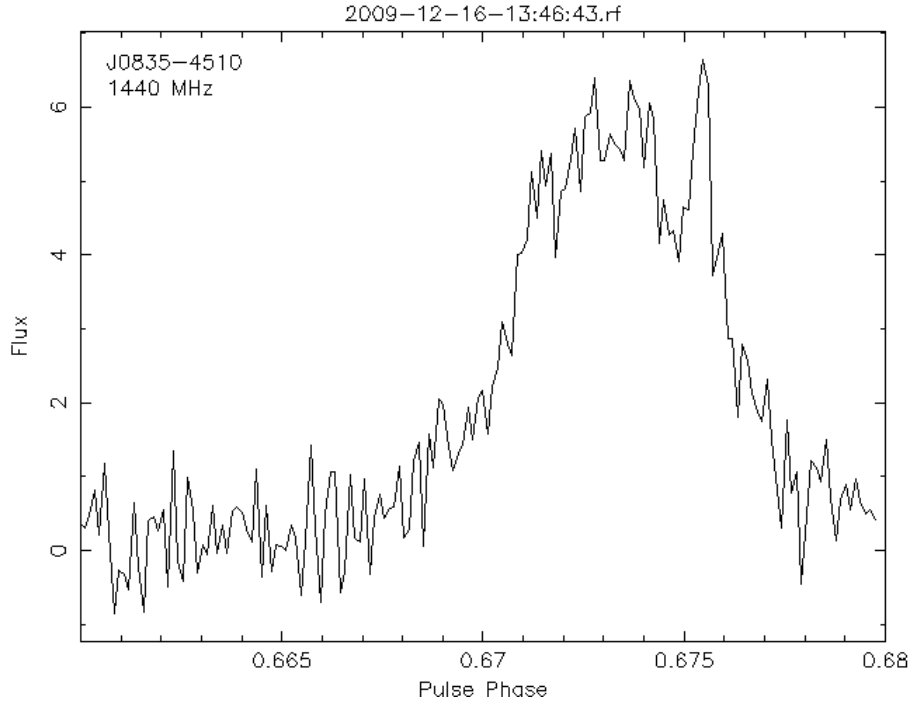

Figure 22: Microstructure for the brightest pulse recorded in the Mt Pleasant data. T-2.

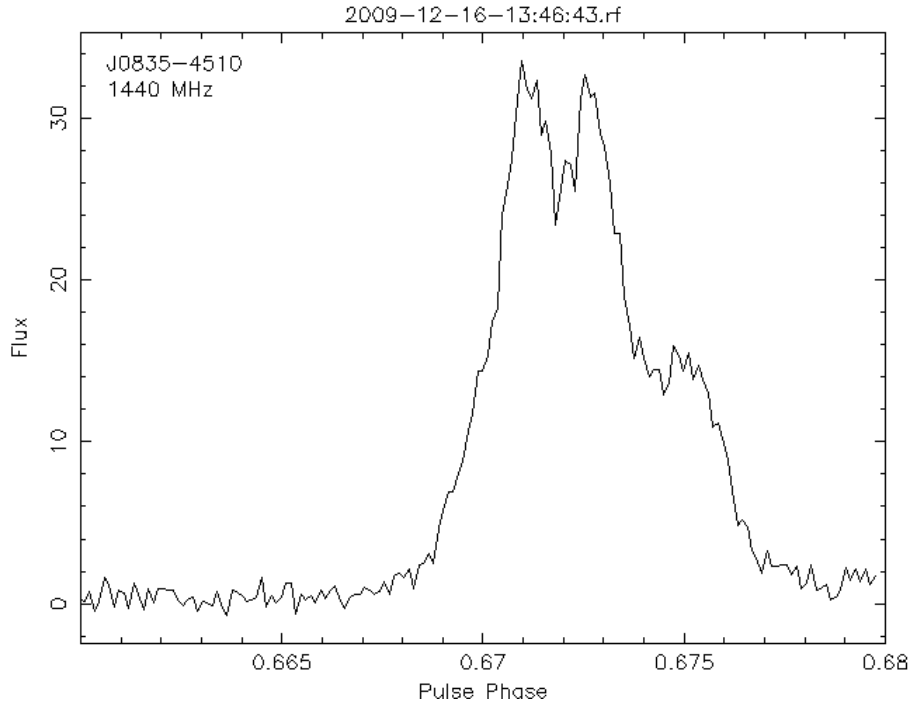

Figure 23: Microstructure for the brightest pulse recorded in the Mt Pleasant data. T-1.

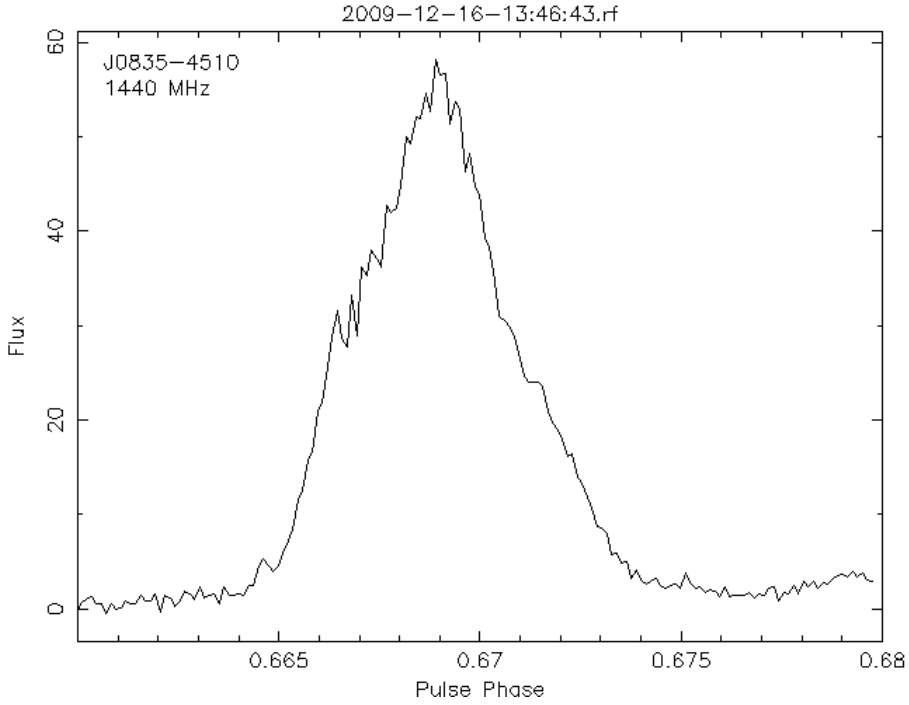

Figure 24: Microstructure for the brightest pulse recorded in the Mt Pleasant data.

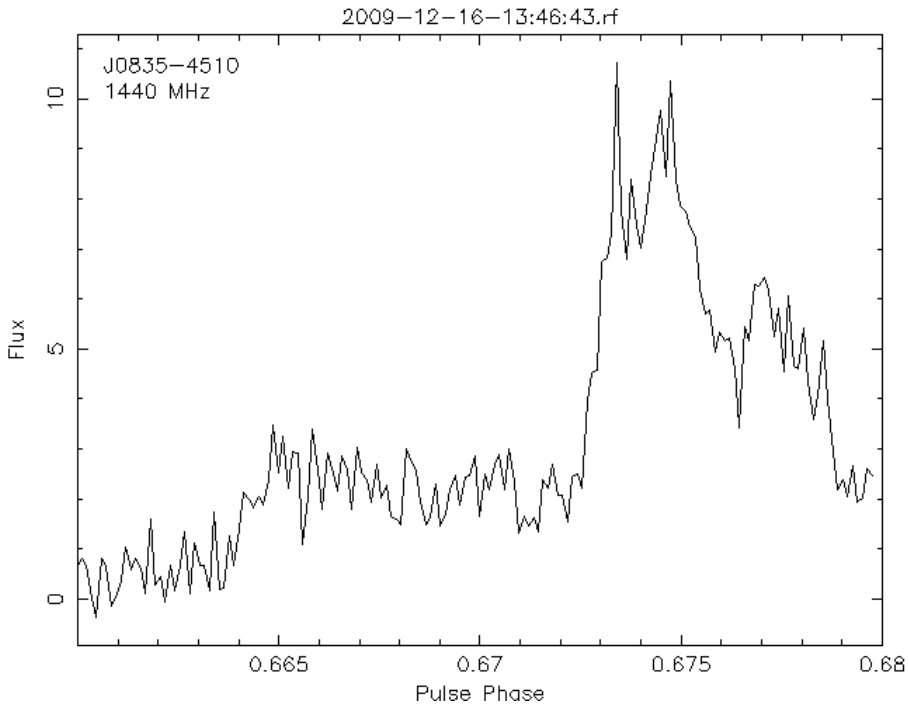

Figure 25: Microstructure for the brightest pulse recorded in the Mt Pleasant data. T+1.

Note the change in phase of each peak - as the pulse gets brighter it appears earlier.

Krishnamohan & Downs (1983) studied the intensity dependence of Vela's pulse profile in detail. They conclude that the pulse profile is composed of at least three, and possibly four independent components. They further conclude that these four components originate at different distances from the neutron star.

Their method involved dividing the pulses up into 15 categories (referred to as "gates") that depended on the flux density. Each gate was then analysed separately. The pulse profiles in each gate were notably different with the lowest gates having two clear peaks and the highest gates having a single peak. Also, the higher the gate the earlier the pulse occurred. Note that our definition of a bright pulse approximately lines up with their three highest gates: 13, 14, and 15.

Also noted in the paper was the change in pulse profile at different frequencies. The trailing component is barely present at 400 MHz, but yet overtakes the main component at 4.8 GHz.

Now the interesting phenomenon of bright pulses appearing consecutively was noticed early on in our investigation. Figure 26 is the first such observation, magnified:

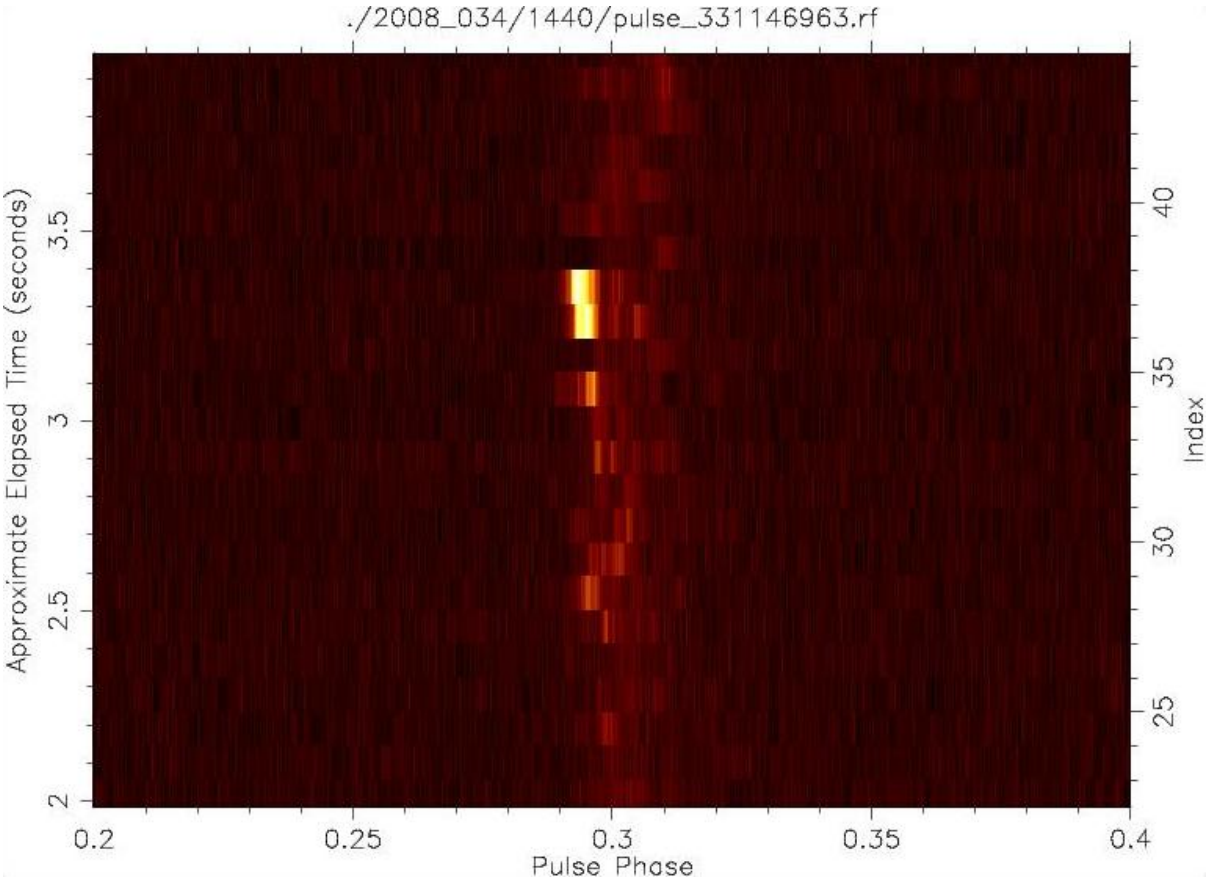

Figure 26: The first consecutive bright pulses discovered in our data.

Again, notice the brighter pulses tend to appear earlier in phase than the main pulse. The Parkes data also had some significant bright pulses, and one that stands out is shown in Figure 27 to Figure 32. Again, y scale varies to show microstructure, but the time axis is fixed.

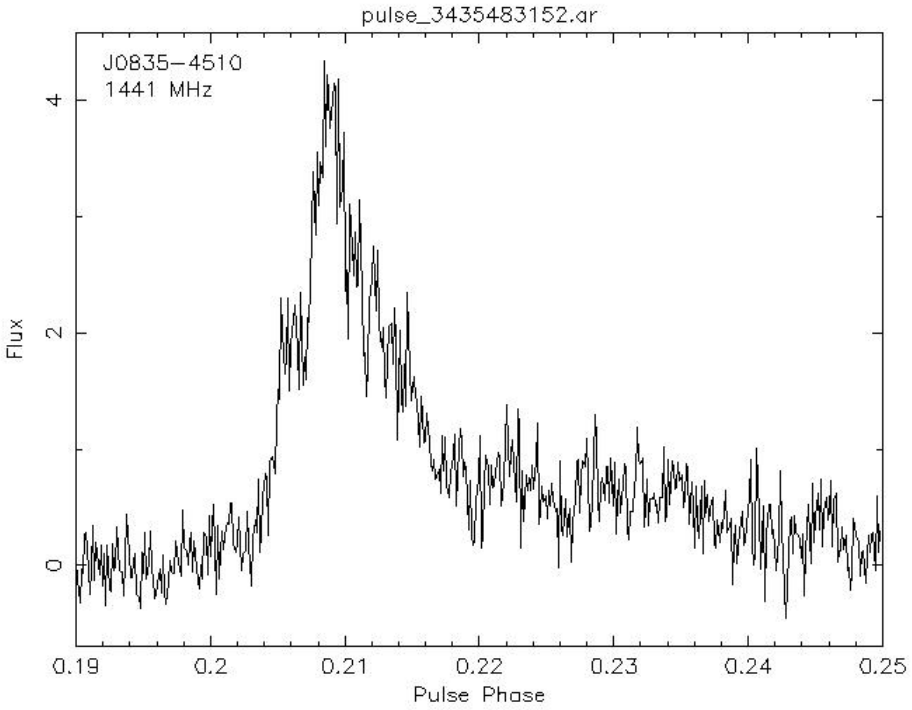

Figure 27: Microstructure for the brightest pulse recorded in the Parkes data. T-3.

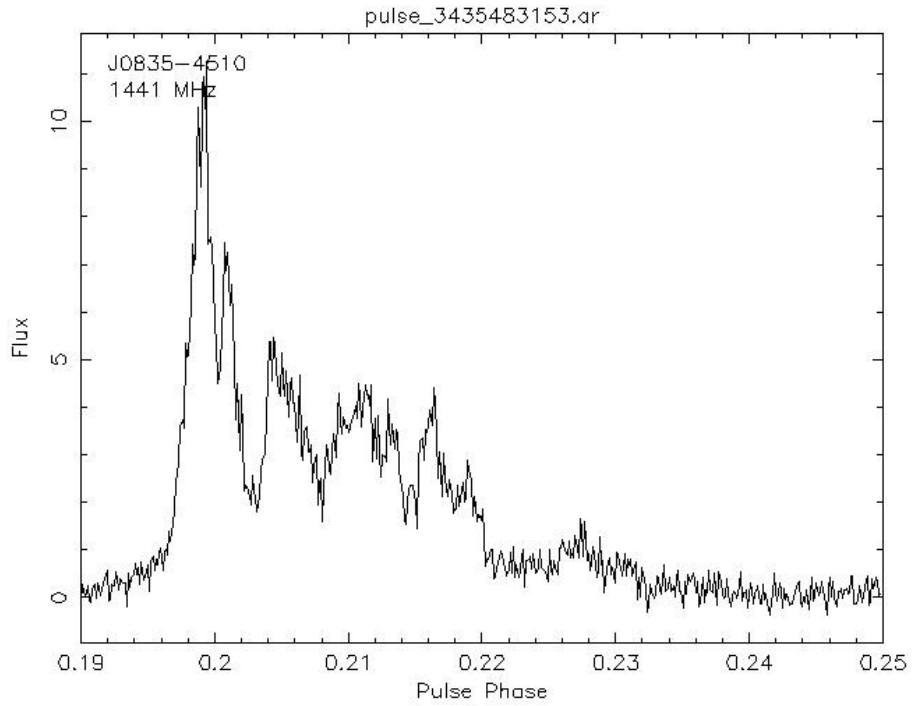

Figure 28: Microstructure for the brightest pulse recorded in the Parkes data. T-2.

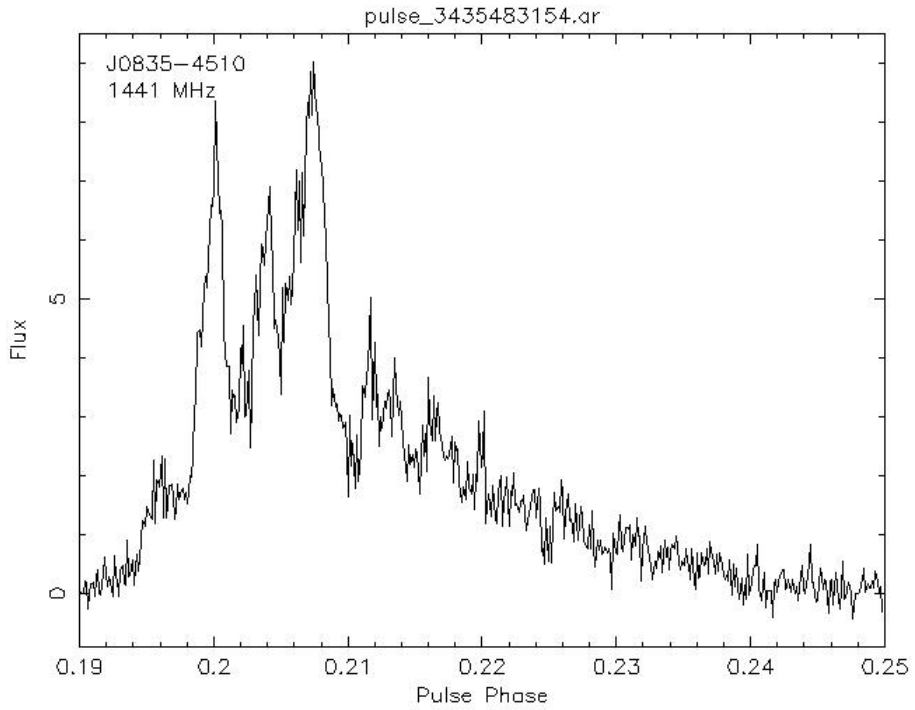

Figure 29: Microstructure for the brightest pulse recorded in the Parkes data. T-1.

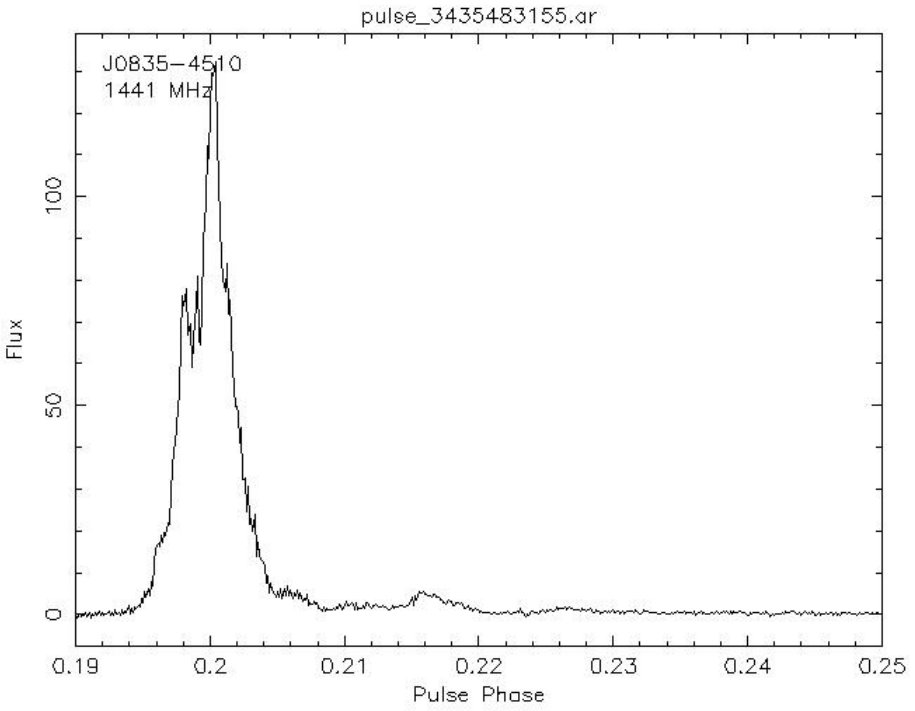

Figure 30: Microstructure for the brightest pulse recorded in the Parkes data.

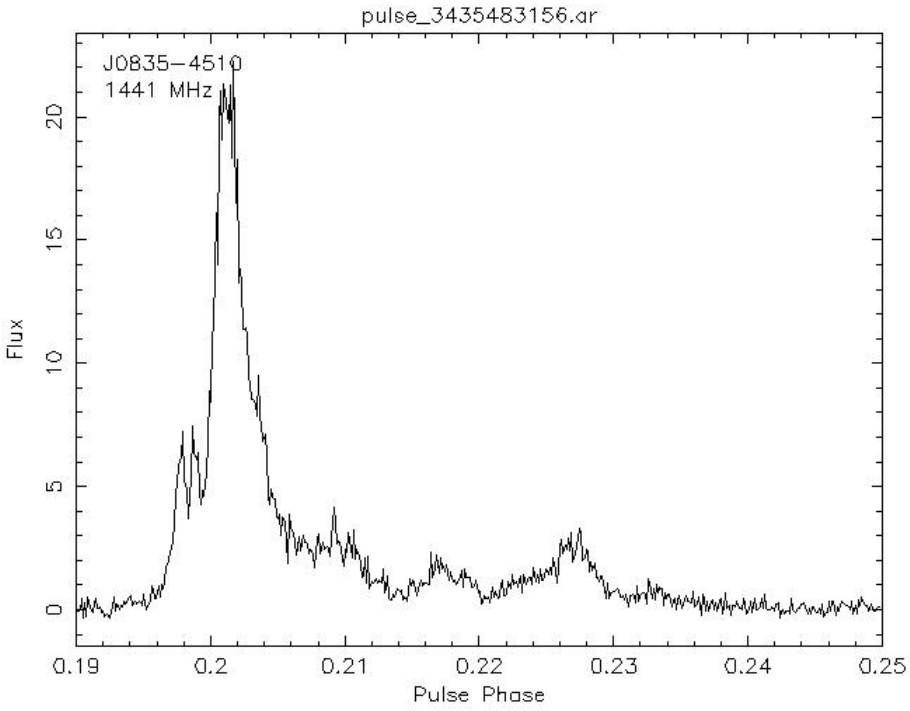

Figure 31: Microstructure for the brightest pulse recorded in the Parkes data. T+1.

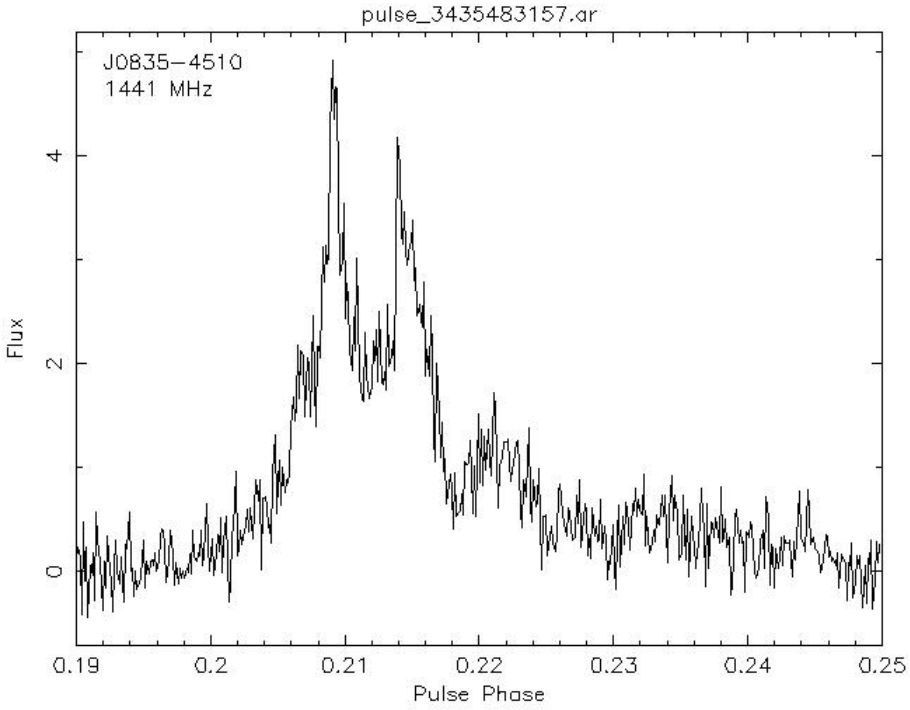

Figure 32: Microstructure for the brightest pulse recorded in the Parkes data. T+2.

5.2. Consecutive Bright Pulses and the Consequences for Emission Hypotheses

Figure 33 shows the first and one of the most interesting discoveries of this search: a series of six consecutive bright sub-pulses that started at 2008 June 29 07:32:20.9823 UTC. The bright sub-pulses are shown starting approximately one second from the bottom. A magnified view of these pulses is shown as an inset.

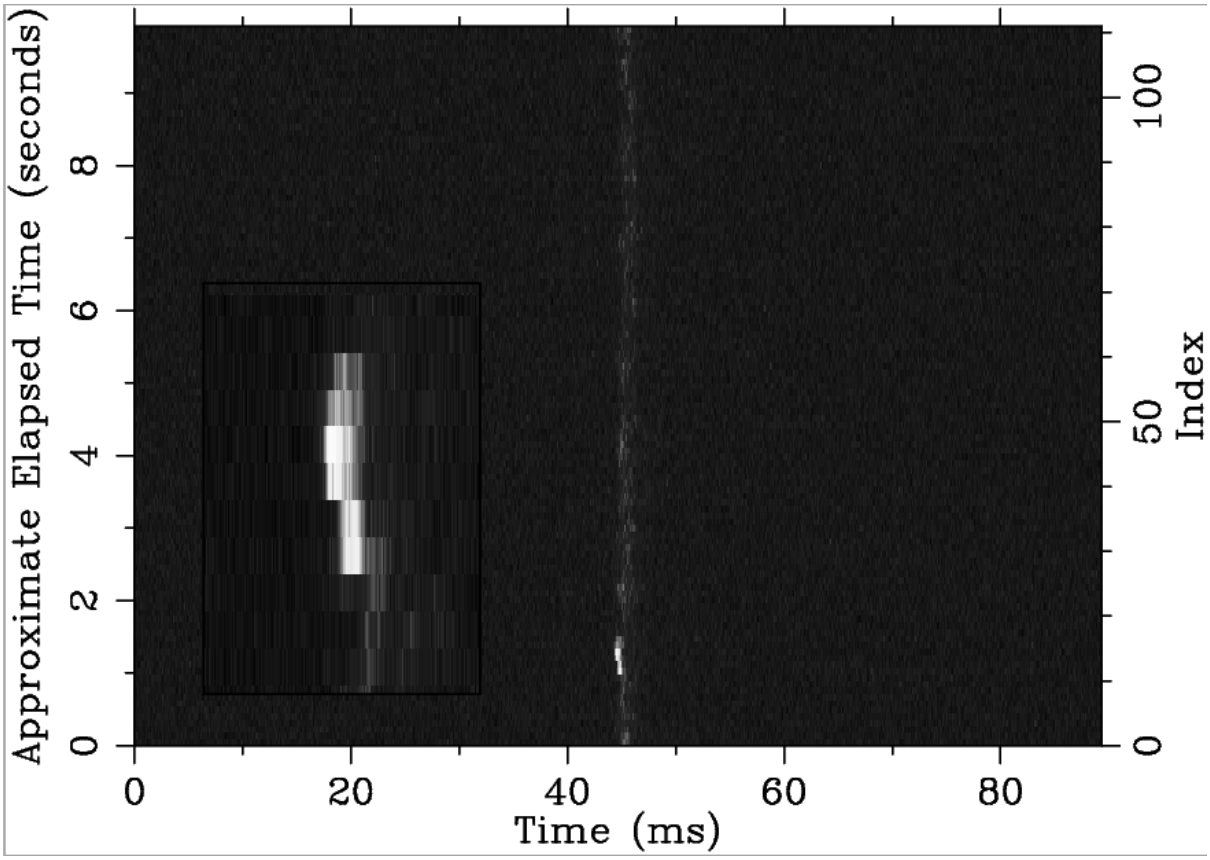

Figure 33: Six consecutive bright pulses seen at 2008 June 29 07:32:20.9823 UTC.

Figure 34 shows flux density vs time for each of these six bright sub-pulses with high resolution in pulse longitude.

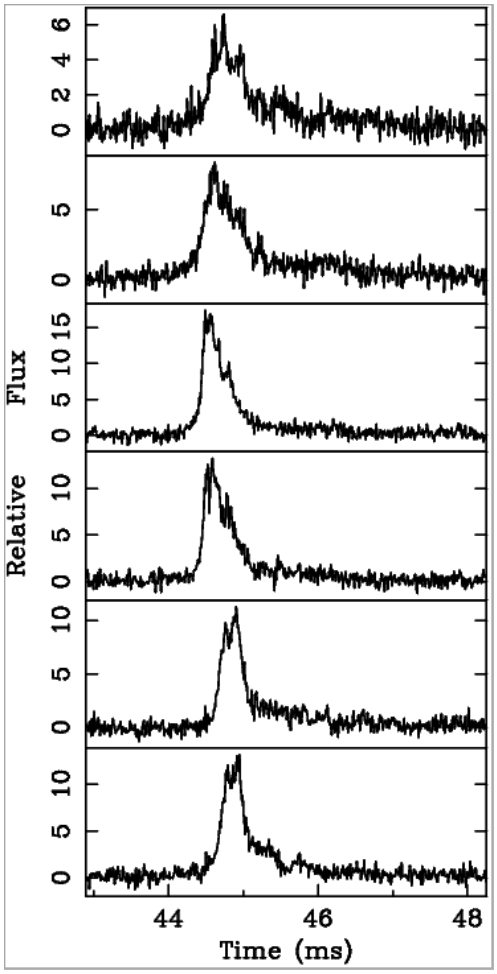

Figure 34: Plot of flux density vs phase for each of the consecutive bright pulses. Note the y scale varies and the pulses are in the same order as Figure 33. The average pulse profile has a peak around 1 on this scale and a width of about 5ms.

Consecutive bright sub-pulses have not been discussed in the literature. They may give an indication of the nature of the pulsar emission process. The fact that they can last a number of pulsar rotations and in this case a total time of 0.5 s is significant. The six bright sub-pulses all occur at a similar longitude, in the leading edge of the pulse (as nearly all bright

pulses in Vela do), and they show similar profiles, with a sharp leading edge and more gradual decrease after the peak.

Events with time scales around 0.5 s have not been previously noted in the Vela pulsar. Consecutive bright pulses of lesser length (i.e. 2, 3, 4 or 5 bright pulses in a row) were also noted in all data sets and were much more frequent (see Table 2).

Consecutive Pulses (n)	Dec 2009 Number Expected (q)	Dec 2009 Actually Observed	2010 Number Expected (q)	2010 Actually Observed
1	22916	22916	5364	10196
2	133	191	30	578
3	0.74	70	0.17	27
4	4.1×10^{-3}	26	0.92×10^{-3}	5
5	23×10^{-6}	10	5.1×10^{-6}	1
6	127×10^{-9}	1	28×10^{-9}	0

Table 2: Expected consecutive pulses vs observed. See text.

Interstellar scintillation could cause amplification of a pulsar signal over short time periods. The NE2001 electron density model (Cordes & Lazio 2002) in the direction of the Vela pulsar predicts pulse broadening of 1.2 μs, a scintillation bandwidth of greater than 30 kHz and a scintillation time scale around 30 s. Since the expected time scale of amplification by scintillation is 60 times longer than the sequence of bright pulses, it is very unlikely that the bright pulses are an effect of propagation of the signal through the interstellar medium. The bright pulse sequences must be intrinsic to the pulsar emission mechanism or propagation through the pulsar's own magnetospheric plasma.

The random chance of consecutive bright sub-pulses occurring, if there were no correlation in the emission process can be easily calculated. A single bright sub-pulse occurs in the Dec

2009 observations with a probability p=0.0053 (once every 190 pulses). Labelling n as the number of consecutive pulses and m the total number of pulses observed, the expected number q of n consecutive bright pulses, if they are uncorrelated, is:

$$q\sim=2(1-p)p^n+(m-n-1)(1-p)^2p^n \quad (1)$$

Note that equation (1) does not take into account the boundary condition of sequential pulses at the very start or very end of the observation, and so will be more and more inaccurate as m approaches n. Now for very large m and small p this simplifies even more to:

$$q\sim=mp^n \quad (2)$$

Results for the number of consecutive bright pulses in the 108 hours of observations from the 13 day campaign in Dec 2009 and the total of 24.22 hours observed in 12 sessions in 2010 are given separately on Table 2.

In the Dec 2009 results, 191 sequences of two consecutive bright pulses are detected. This is notably higher than the prediction of equation 1, which is 133. For n=3 we expect to see fewer than one sequence in 108 hours of observations, but we find 70. With n=4,5,6 there are several sequences detected, although the expected number based on equation 1 is very small (columns 2 vs 3 and 4 vs 5, Table 2).

Results of the 24.22 hours of observations in 2010 are shown in columns 4 and 5 on the table. Another sequence of six consecutive bright pulses was not detected, but the shorter sequences of consecutive bright pulses were detected in numbers consistent with the

results of the December 2009 campaign. The ratio of bright pulses to all pulses was 1/190 for the Dec 2009 observations and during the first half of 2010.

Vela “glitched” on 2010-07-31 (Buchner, 2010). After the glitch the bright pulse rate increased to 1/111. This change in bright pulse statistics after the glitch, and the variation with time of the pulse height distribution, is discussed more in-depth in Chapter 7.

To see if the bright pulse statistics were sensitive to the arbitrary choice of threshold (five times the mean flux density), we re-calculated the statistics using a lower threshold. As expected, many more “bright” pulses and consecutive bright pulses were found with a lower threshold, and the probabilities were still many orders of magnitude under what was observed.

Our conclusion is that the hypothesis that bright pulses are independent events is ruled out. The high incidence of bright pulse sequences shows that the physical process causing bright pulses is long-lived relative to the pulsar rotation rate.

5.3. Parkes Data Confirmation

With unique observations from a single telescope there is always a slight doubt that it is a local instrument issue. Gathering data from another telescope can resolve this doubt. Our attempts to confirm the results using the Ceduna 30 m telescope unfortunately did not occur due to the DSPSR software bug.

However, as stated earlier we were fortunate enough to receive an hour’s worth of single pulse data from the Parkes 64 m radio telescope.

We selected the bright pulse cut-off at 30 (above which had under 2% of the pulses – roughly the same as the Mt Pleasant results) and on average had a probability of 0.00895 of occurring.

At this level (assuming independence of bright pulses), we would have expected to see 3 doubles, 0.03 triples and 2.76×10^{-4} quadruples in that observation, and yet we found 11, 1, and 1 respectively. Note that even though we only had about an hour's worth of data, we were lucky enough to get a quadruple consecutive bright pulse. This is a solid confirmation that the observations at Mt Pleasant were not location specific.

Capturing a quadruple pulse at multiple frequencies is also useful. Shown below in Figure 35 and Figure 36 is the quadruple pulse in the time vs time graph.

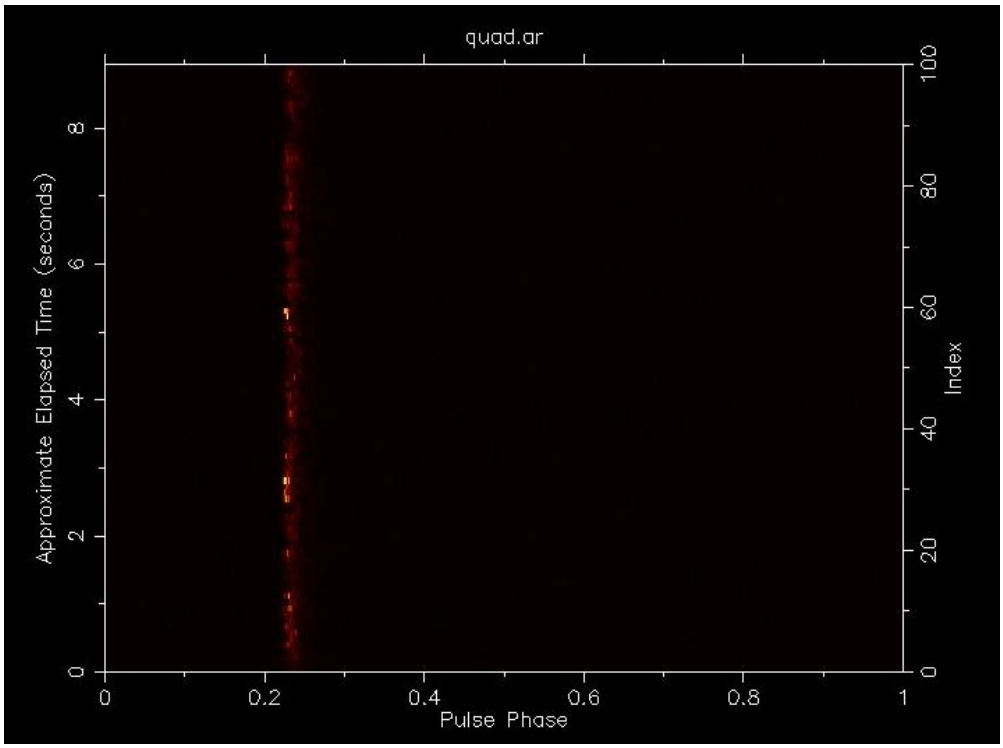

Figure 35: Time vs time graph of the quadruple pulse recorded at Parkes.

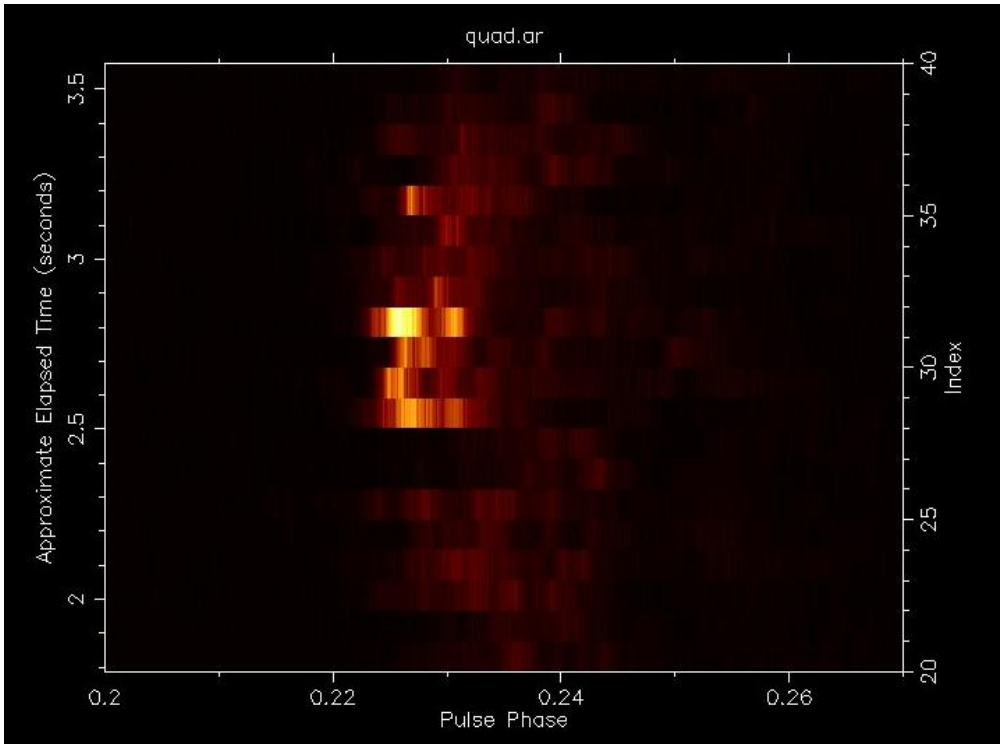

Figure 36: Same as previous, but magnified. Note the dark area in the two pulses leading up to the consecutive bright pulses.

What stands out in this diagram is the “black patch” just prior to the consecutive pulses. Comparing this with the Mt Pleasant data (see magnified Figure 21, Figure 26, and Figure 33), similar low emission prior to the large pulse seems to occur – just less noticeable due to instrument noise. If there is indeed a hole in the magnetosphere letting radiation through, maybe the surrounds of the hole are denser (if it is a spinning vortex like the eye of a cyclone perhaps).

The following eight figures are of the four individual pulses at 1249 MHz (the lowest available in the Parkes data) and 1441 MHz (very close to our Mt Pleasant frequency). Note the y scale varies (to capture all the fine detail) and the x scale is fixed.

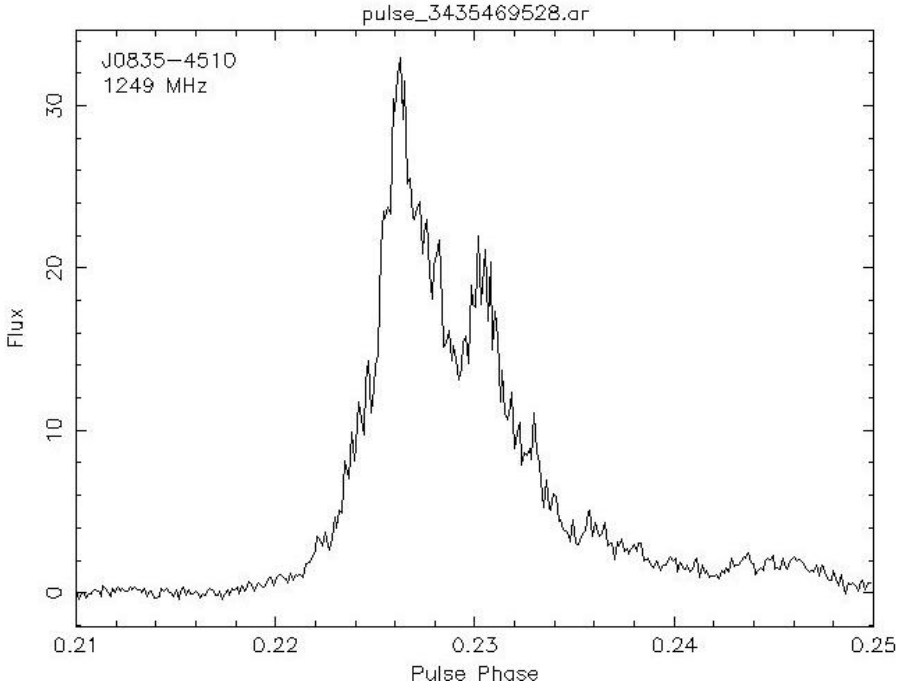

Figure 37: Pulse 1 of 4 at 1249 MHz.

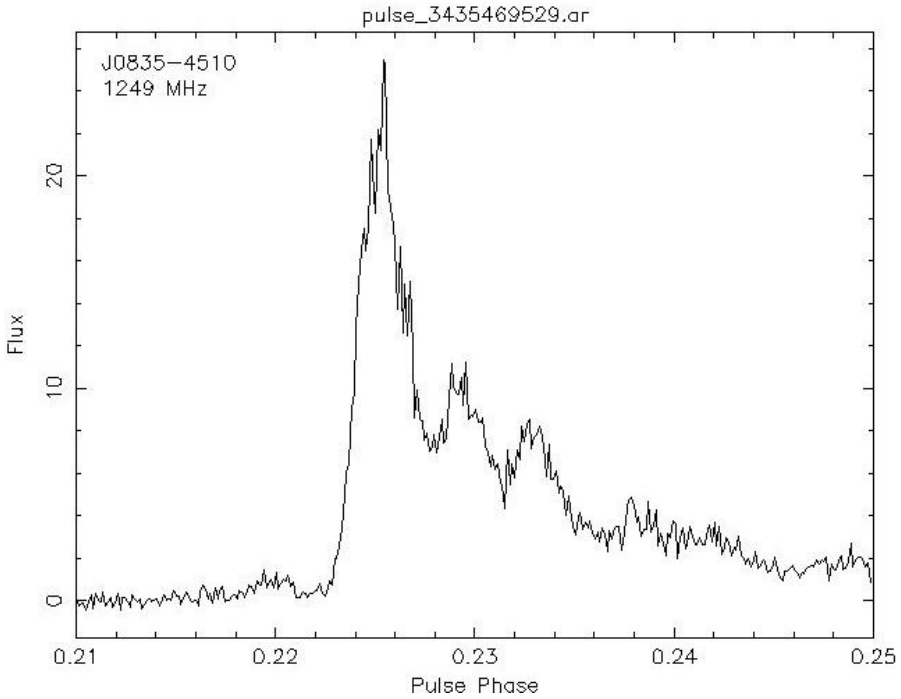

Figure 38: Pulse 2 of 4 at 1249 MHz.

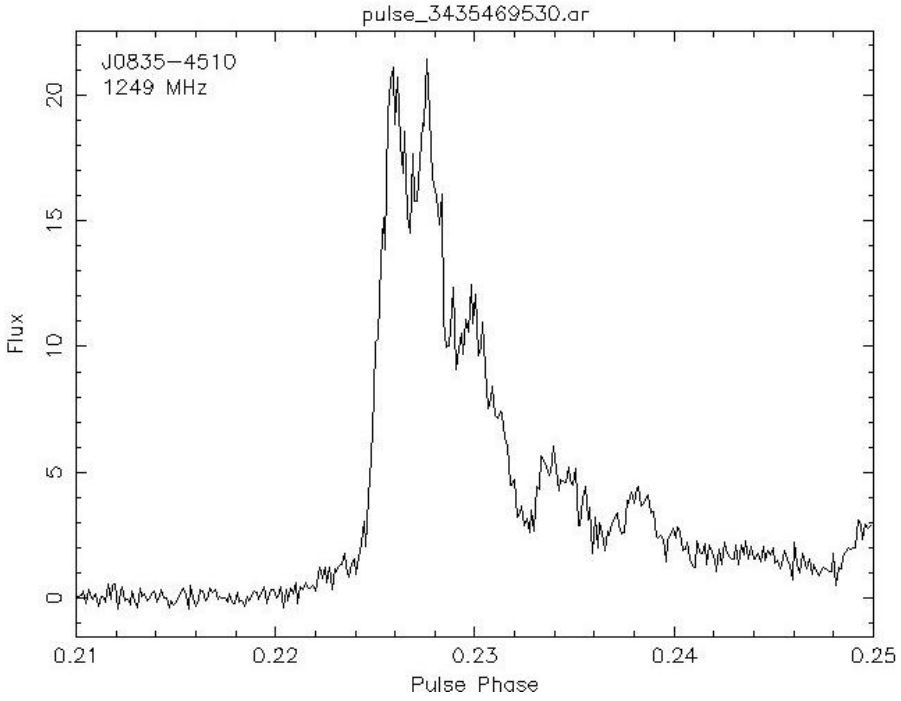

Figure 39: Pulse 3 of 4 at 1249 MHz.

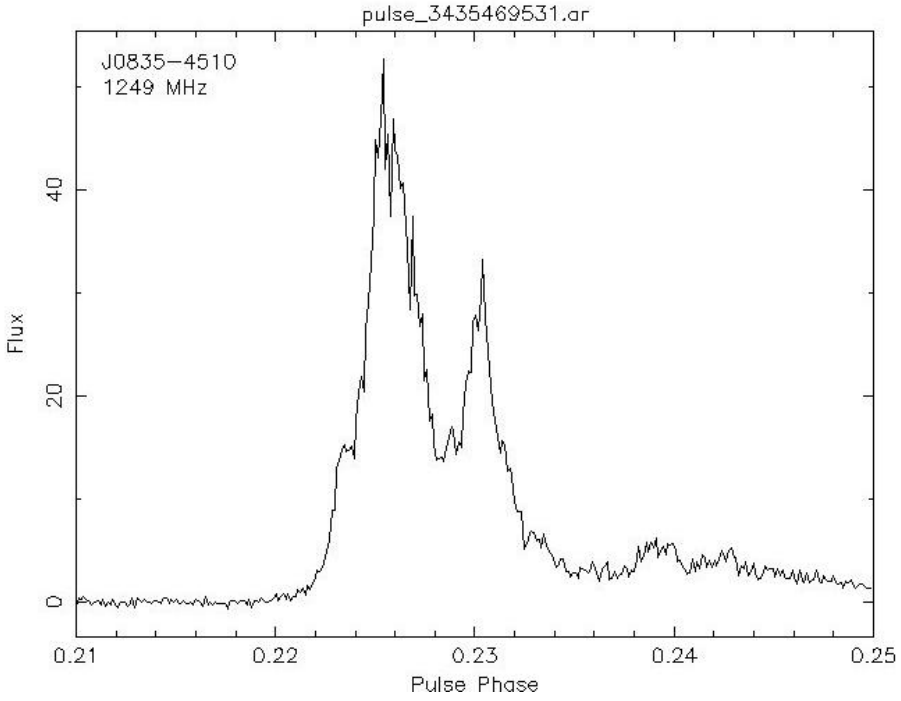

Figure 40: Pulse 4 of 4 at 1249 MHz.

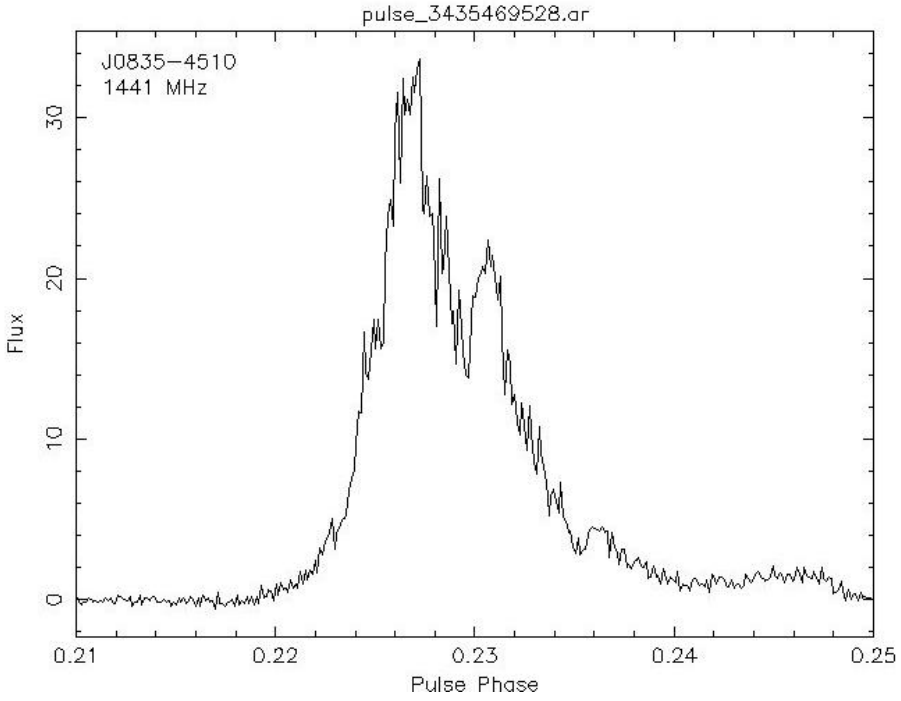

Figure 41: Pulse 1 of 4 at 1441 MHz.

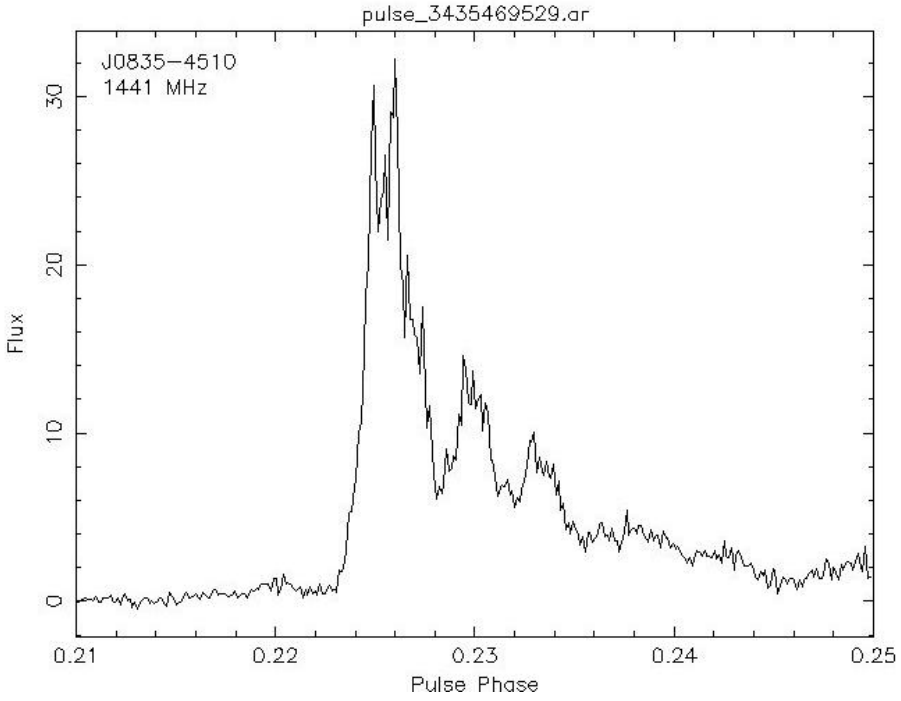

Figure 42: Pulse 2 of 4 at 1441 MHz.

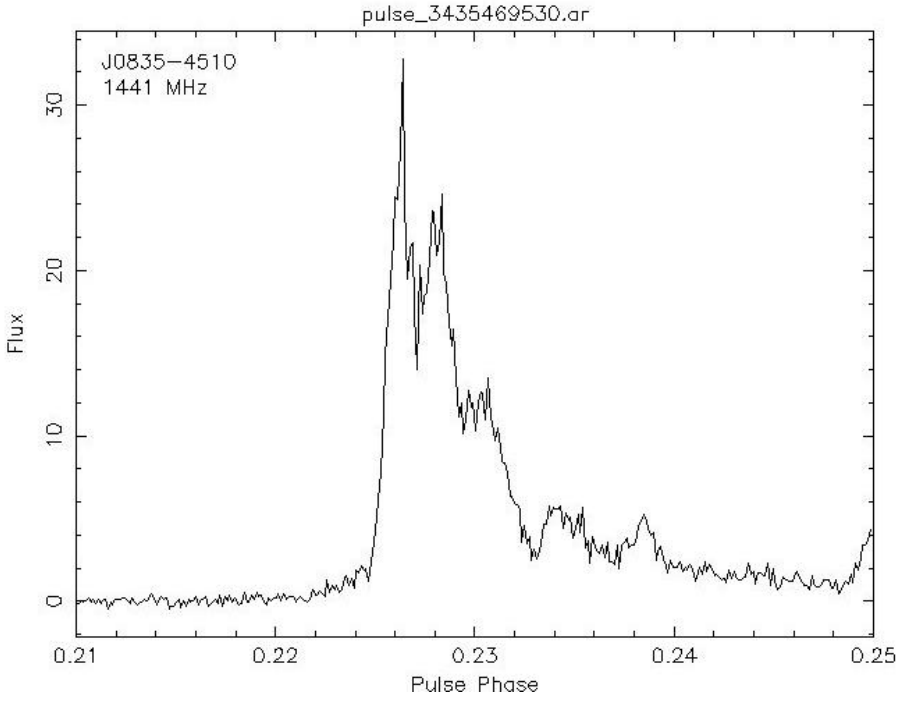

Figure 43: Pulse 3 of 4 at 1441 MHz.

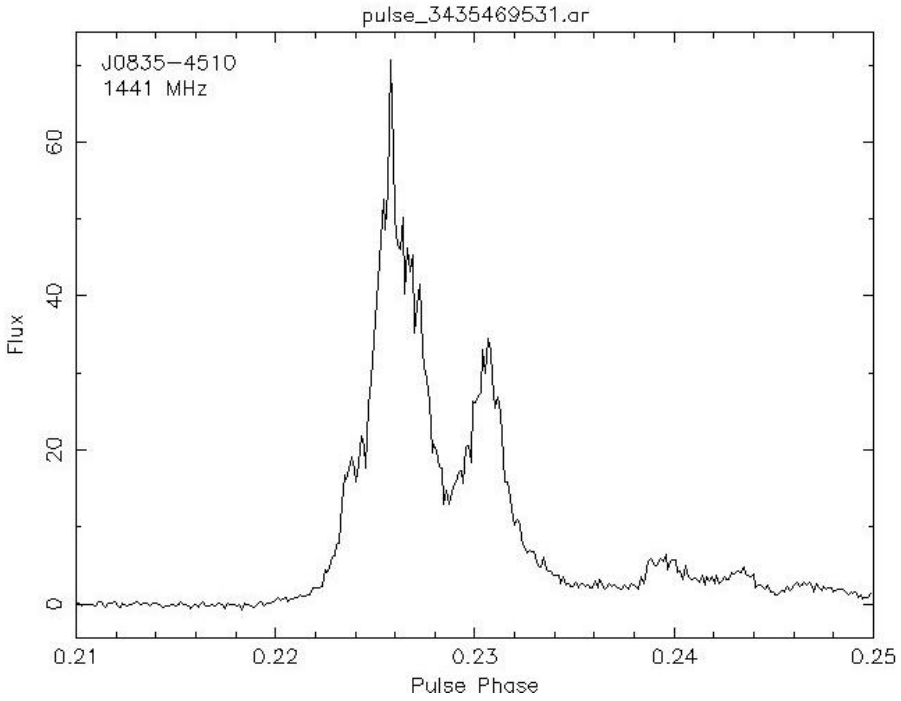

Figure 44: Pulse 4 of 4 at 1441 MHz.

Pulse 2 is intriguing. Note the multiple decreasing peaks, equally separated. If Kontorovich is correct and this is a gap in the magnetosphere, it is conceivable that this is Fraunhofer diffraction caused by viewing radiation through the hole from a distance. The separation of the peaks (or troughs) in Fraunhofer diffraction, as an angle, for a given wavelength, is given by:

$$\tan\theta = \left(\frac{\lambda}{a}\right)$$

where *a* is the diameter of the aperture.

Magnifying the view of this pulse and looking at the highest and lowest frequency range from Parkes we get Figure 45 and Figure 46.

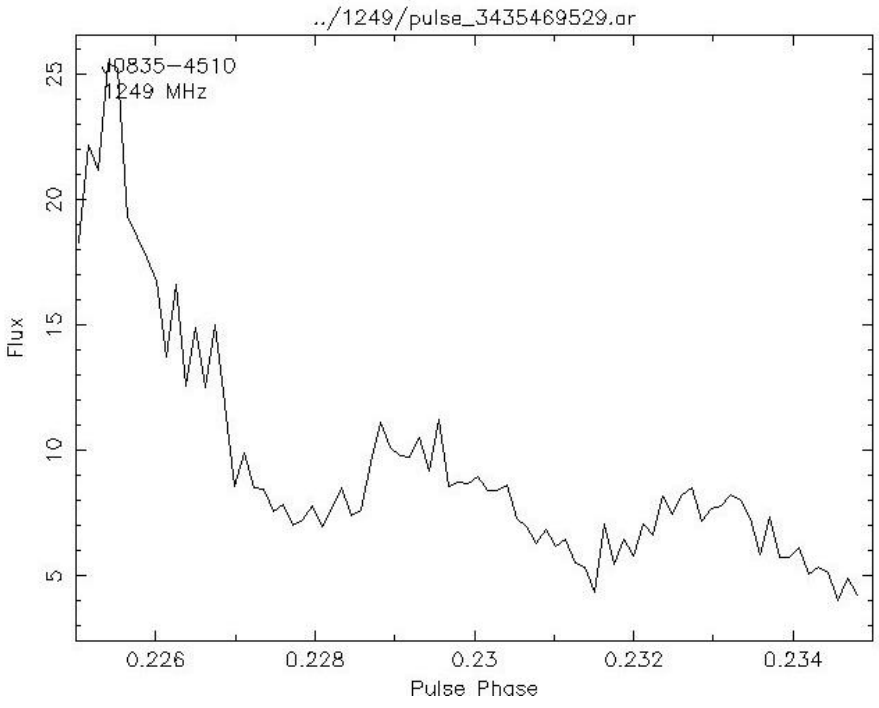

Figure 45: Magnified view of potential Fraunhofer diffraction at 1249 MHz.

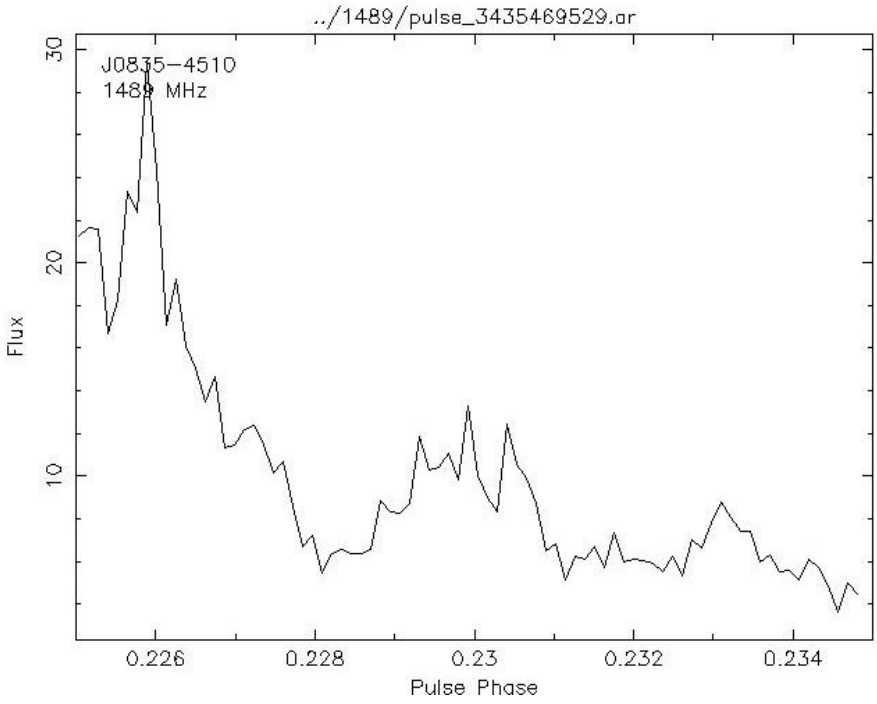

Figure 46: Magnified view of potential Fraunhofer diffraction at 1489 MHz.

So if we select 1489 MHz and take from Figure 46 that the distance between the troughs is 0.004 of a period, this means the size of the aperture is:

$$a = \frac{c}{(1489\,\mathrm{x}10^{6})\tan(2\pi(0.004))}$$

where c = 299 792 458 ms^{-1} which is the speed of light. This gives a = 8 m.

The Fraunhofer diffraction equations assume parallel waves striking an aperture or slit. This is unlikely to be the case on a pulsar, and with other high-energy physics and relativistic effects occurring, this result needs much more examination. But the 8 m figure is nonetheless in the bounds of acceptability since from Table 1, the polar cap of Vela is calculated to be 484 m across.

Taking the next step and assuming the aperture is 8 m, then we should be able to calculate the difference in the peaks at the lower frequency at the other end of our band: 1249 MHz. The separation of the peaks/troughs should be:

$$\Delta = \frac{\tan^{-1}\left(\frac{c}{(8)(1249\text{x}10^{6})}\right)}{2\pi}$$

This calculates to 0.00477. This difference is 0.00077 of a period or 68.8 μs and so it is just a bit too small to reliably compare with the data we have in Figure 45.

Note that Figure 28 also exhibits this phenomenon.

Interestingly, Ables et al. (1997) also found:

> *"a periodic fringe structure...strongly reminiscent of the diffraction pattern of a sharply bounded finite aperture"*

in J0437-4715. Their conclusion for the observation is a thin charge sheet of diameter 110 m but only emitting on a charge annulus of 7 m. Now their emission model is quite different to Kontorovich, but it is interesting to note that the actual diameter of the emission area (8 m and 7 m respectively) match quite nicely.

These require further observations and investigation. It is possible these diffraction patterns could be used to discover more information on the nature of the emissions from pulsars.

---

6. Confirmation of Giant Micro Pulses

Johnston et al (2001) showed the occurrence of “giant micro pulses” in the Vela pulsar. As stated earlier, these are pulses that have a large peak flux density, but are very narrow (<500 µs). The paper notes the brightest pulse as one which is 40 times the peak flux density of the mean pulse and has a FWHM of ~400 µs. It also notes two extremely narrow (50 µs) pulses – but the highest of these has a peak of 6 times the mean pulse.

Our algorithm for calculating the width of pulses (see Chapter 4.3) was not perfect in that for multiple peaks the total pulse width would not be technically correct – only the highest peak would be measured (at its halfway point). However, it should be very sensitive to high narrow pulses and so this was the reason it was adopted.

Figure 47 is a plot of Flux Density vs Pulse Width from all our valid Mt Pleasant observations in 2009/2010.

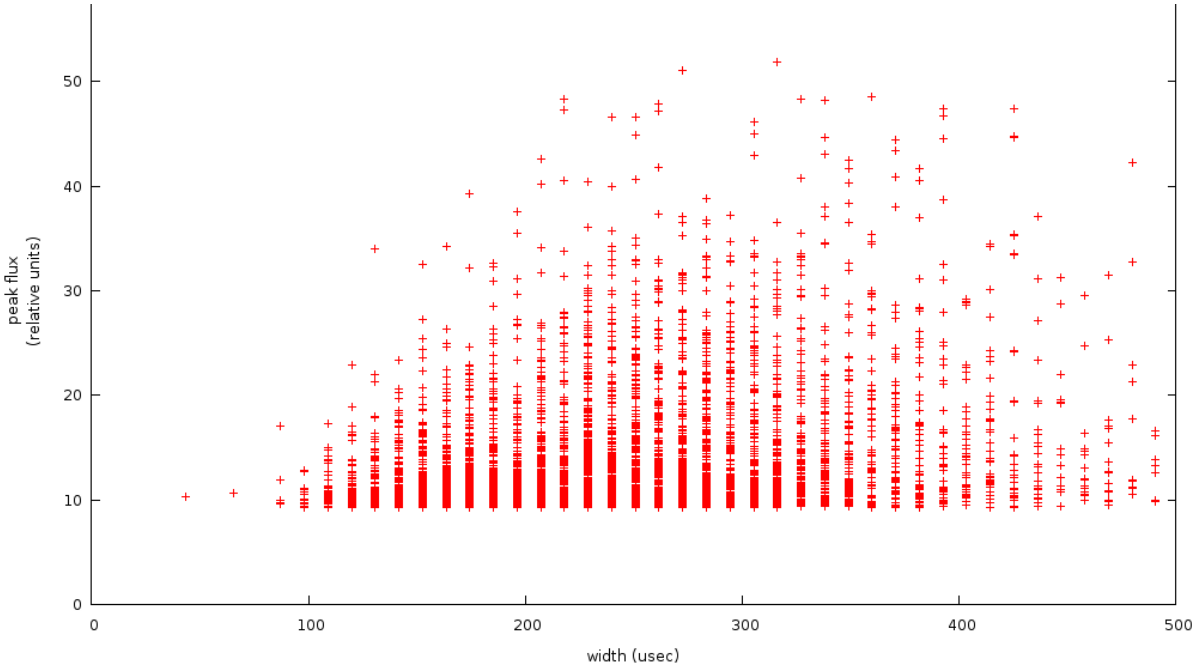

Figure 47: Peak flux density vs width for bright pulses prior to July 31 2010. (i.e. not including the post glitch data - see Chapter 7).

Giant micro pulses (high flux density and a width of under 500 μs) are significant. Since our observations at Mt Pleasant had a resolution of 10.9 μs and Johnston only had a resolution of 44 μs, it is expected we should have detected these.

Johnston's team used the 64 m Parkes radio telescope and so we also analysed our Parkes data – and got a similar result which is shown in Figure 48.

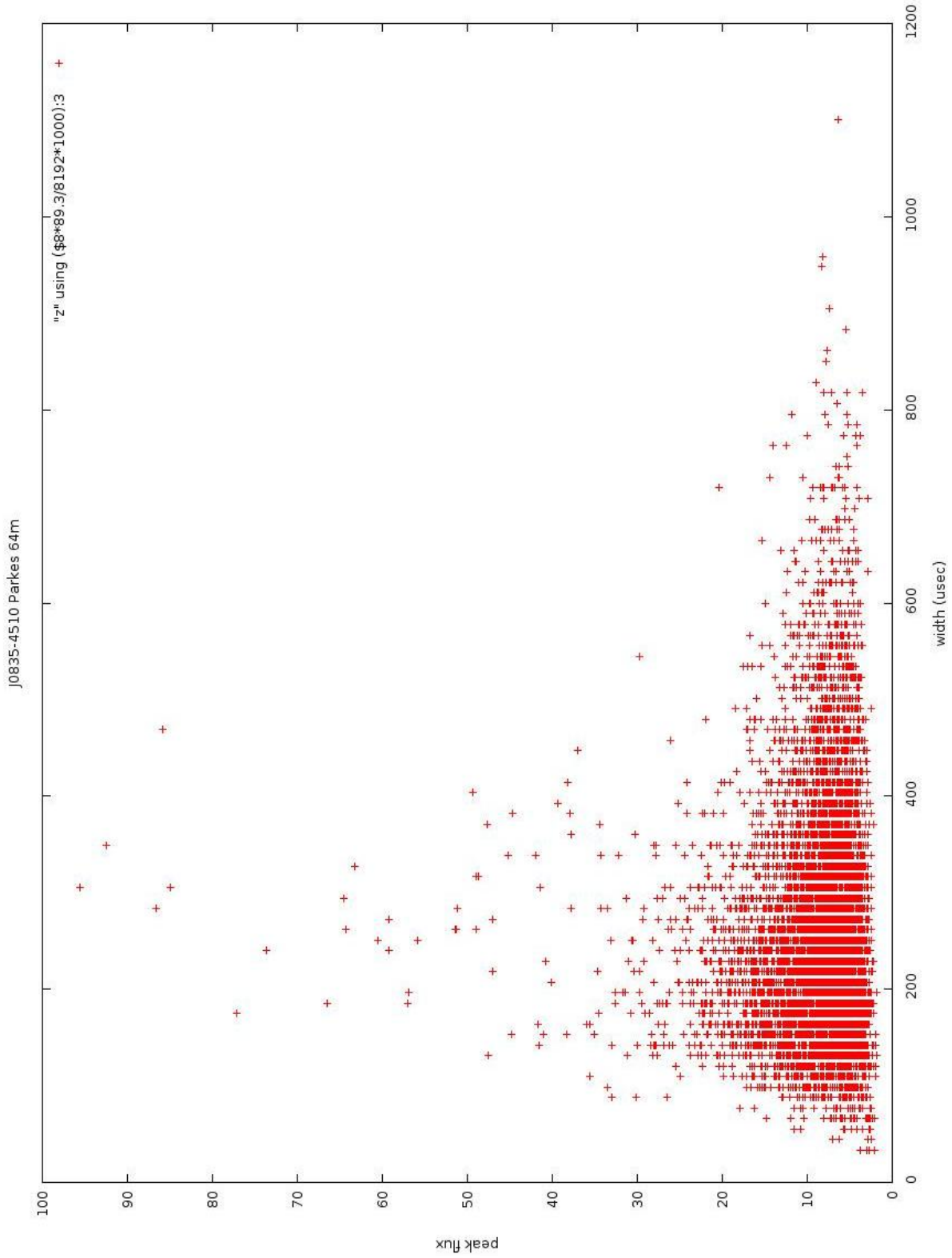

Figure 48: Scatterplot of peak flux density vs width for approximately 40000 pulses from the 64 m telescope at Parkes. The average pulse is at 4.1 on this scale.

There is a significant hump at around the 200 μs width and some of the flux densities peak around 30 times the average peak. Even down at the 50 μs level, there are a number of pulses at around 4 times the average pulse. Keeping in mind that the Parkes data is only 1 hour, and Johnston's data is about 30 minutes, variations are to be expected.

---

7. Glitches and their possible Effects on Bright Pulses

Interestingly, in all of the current glitch hypotheses and under current emission models, one would not expect glitches to affect the frequency of bright pulses. The increase in rotation frequency of Vela is typically of the order of 2×10^{-6} ss^{-1} which is quite large and easily measureable from a timing perspective, but is it large or small when considering effects on the surface of the pulsar?

With a radius of 10000 m, hence a diameter of 63000 m and turning 11.2 times per second this means a point on the surface covers ~700000 m in 1 s. A 2×10^{-6} ss^{-1} change would equate to a little over 1 m in 1 s (assuming the change occurred that quickly). Would this have an effect? This requires further study.

On Jul 31.802 UT 2010, Vela glitched. A single four hour observation after the glitch showed the following interesting statistics (see Table 3) when compared to a four hour observation prior to the glitch.

Consecutive Pulses (n)	Bright pulses observed Pre-glitch	Bright pulses observed Post-glitch
1	896	1508
2	28	120
3	2	7
4	0	3

Table 3: Comparison of bright pulses and consecutive bright pulses in two 4 h observations, before and after the glitch on Jul 31.802 UT 2010.

This is a significant increase in the number of both bright pulses and consecutive bright pulses.

To see this in a larger context, Table 4 shows the consecutive bright pulses per count for all observations. These are grouped by telescope and whether they are pre or post glitch.

		Consecutive Bright Pulses per Hour			
Observations	**Bright pulses per hour**	**2**	**3**	**4**	**5**
All 26 m pre-glitch	264	2	0.7	0.25	0.1
Parkes (pre-glitch)	363	10	1	1	-
All 26 m post glitch	542	32	1.6	0.3	0.1

Table 4: Table of consecutive bright pulses per hour of all observations

As can be seen the bright pulses per hour has more than doubled, 2 consecutive bright pulses has jumped enormously, 3 consecutives have doubled. Note that 4 and 5

consecutives stayed roughly the same – although the absolute figures were low in these columns.

Figure 49 shows a plot of bright pulse flux densities against date for a large sample of valid data collected in the years 2009 and 2010 (note we lost the last half of 2008 and first half of 2009 due to the software bug).

Keeping in mind the glitch occurred at the end of July 2010, this figure appears to show an increase in bright pulse activity. Although because of the clusters of observing activity it is still not as clear as it could be. So instead Figure 50 is a histogram of bright pulse counts per minute which does highlight the changes.

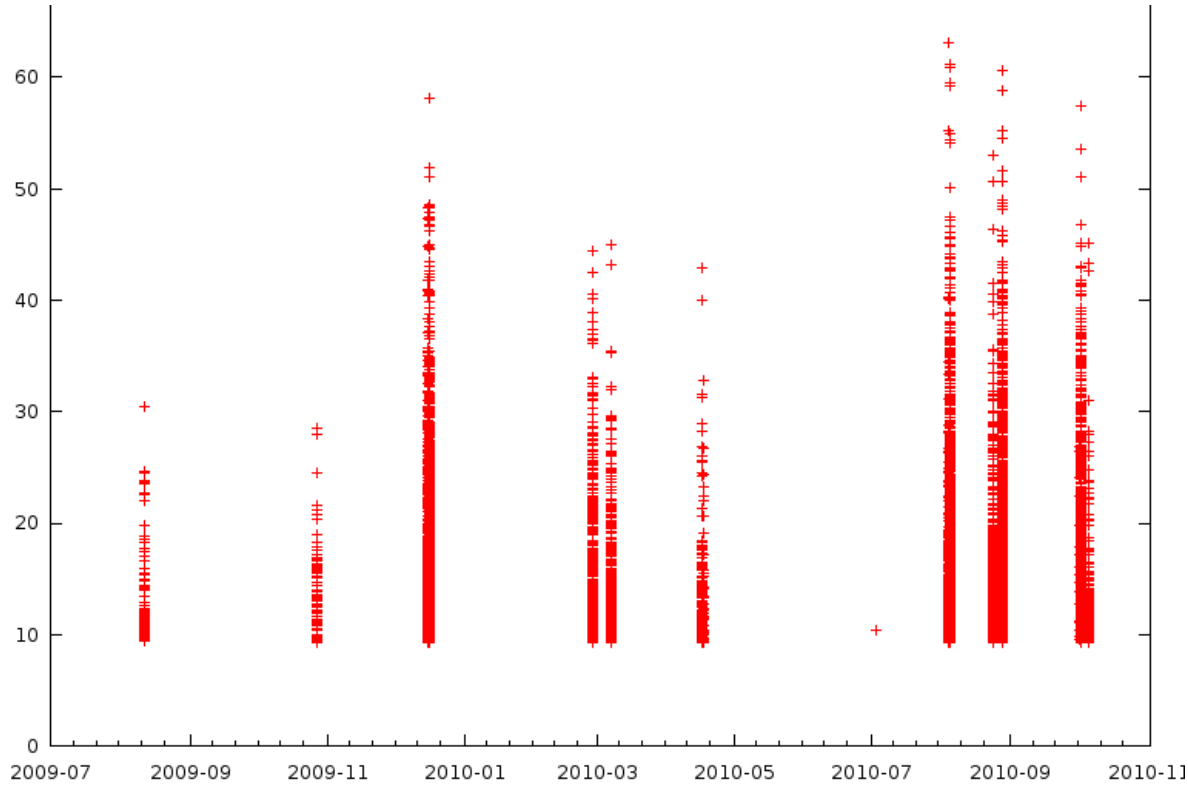

Figure 49: Plot of all bright pulses and their peak flux densities vs observation date. The y-axis is flux density (in relative units) and the x-axis is observation date.

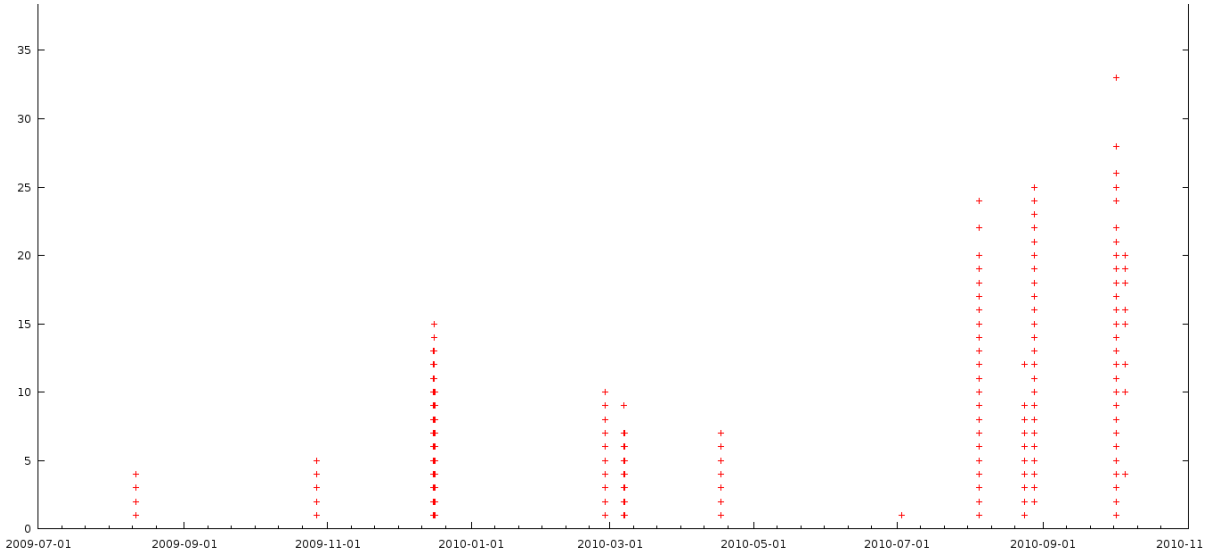

Figure 50: Histogram of a count of bright pulses each observing minute, organised by date.

The clustering of data when representing the x-axis in absolute date format still hides information and so Figure 51 just bins the entire observing-minutes one after the other on the x-axis, with the vertical line marking the glitch.

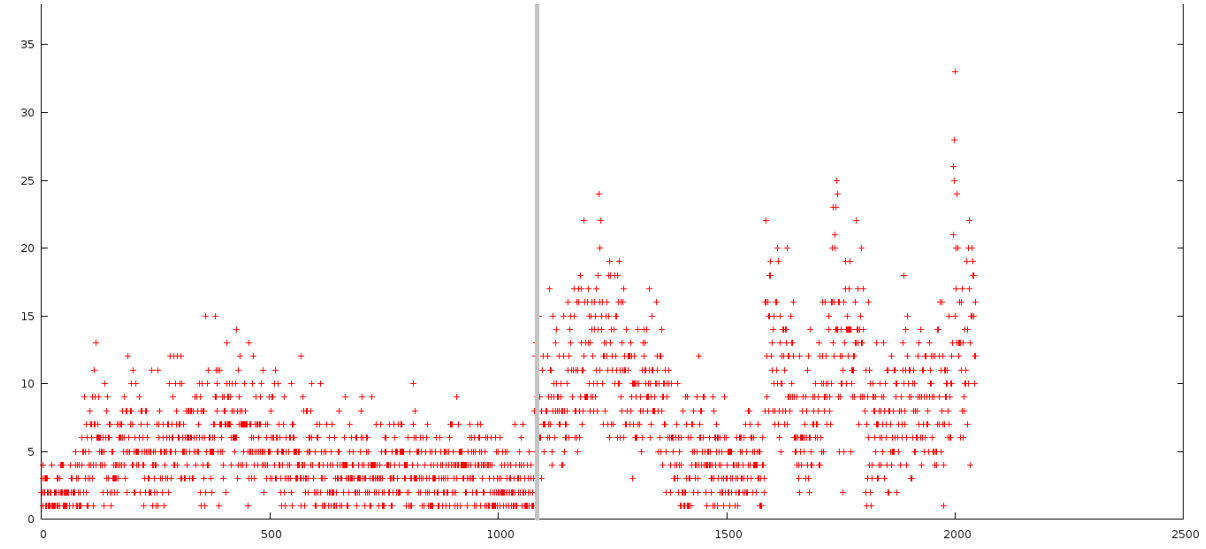

Figure 51: Histogram of bright pulses per observing minute for a selection of pulses before and after the glitch. Each bin on the x-axis is a minute of observing with the y-axis being a count of bright pulses. The verticle grey line marks the glitch.

The change in bright pulse counts after the glitch is quite marked, although it is not sensible to interpret any temporal patterns by using this histogram as the x-axis is not linear.

The mean of the pre-glitch bright pulse rate is 4.4 bright pulses per minute and the post-glitch rate is 9.0 bright pulses per minute. A simple T-Test gives a vanishingly small p-value and so we can conclude that this is not a chance event.

Interestingly when looking at the Flux Density vs Pulse Width plot containing only data after the glitch, we get Figure 52. When compared with Figure 47 there is a noticeable increase in the "area under the curve".

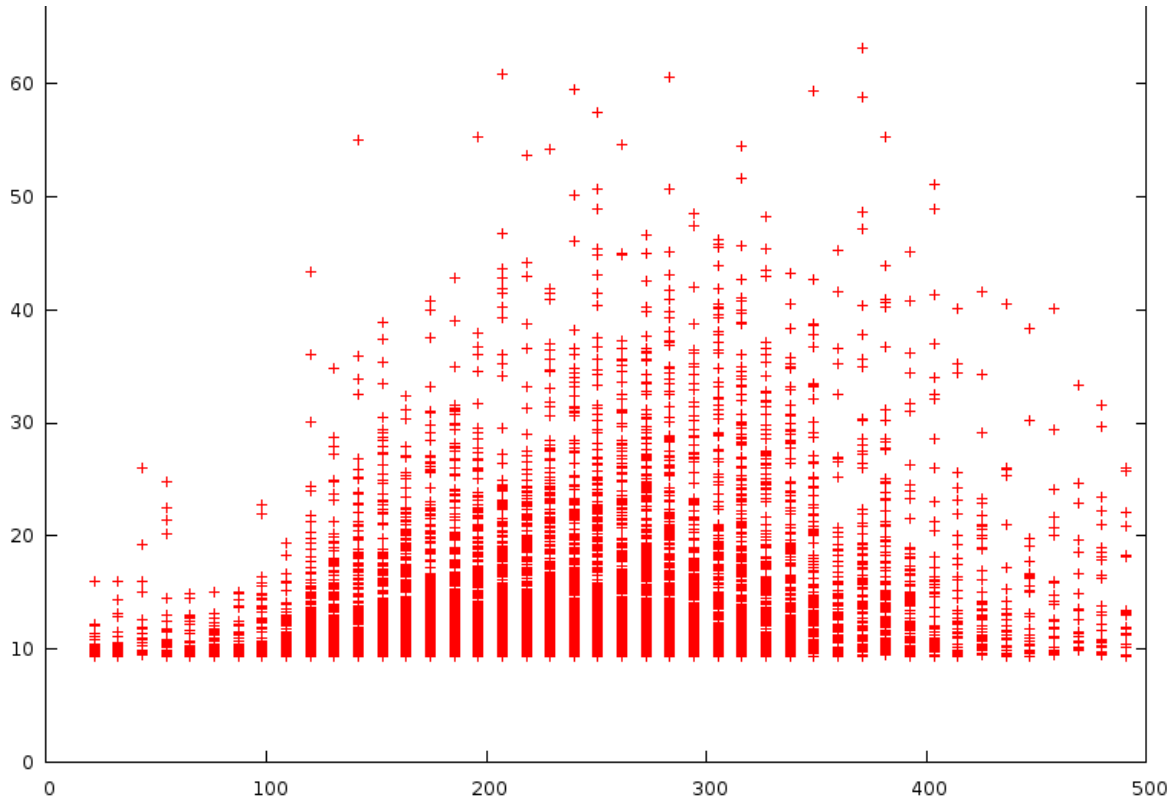

Figure 52: Peak flux density (relative units) vs pulse width (μs) for bright pulses observed after the glitch.

Note that there appears to be a hint of extra bright narrow pulse activity in the sub 50 µs section. Unfortunately after analysis of each individual case, these all turned out to be interference. The positive side is that this showed that the pulse width algorithm was able to adequately detect narrow bright pulses.

The fact that a small change in rotation speed can affect emissions is a bit counter-intuitive with the current popular emission models. However, Kontorovich's model, which has bright pulses as gaps in the magnetosphere, would only need the glitch to cause a temporary turbulence in the magnetosphere which settles down after time passes. There is plenty of scope for further research here.

8.Conclusion

8.1. Summary

We currently have, as of this writing, the longest single-pulse study of any pulsar anywhere in the world. This thesis has only examined the tip of the iceberg with regard to the data obtained. From this examination, we have identified large sequences of consecutive bright pulses that challenge some current emission hypotheses.

These models are generally focused on the emission of the standard pulse and do not take into account the nature of bright or giant pulses.

Karastergiou and Johnston's (2007) empirical model for beams modifies the patchy beam structure by having different emission heights and different numbers of emitting patches per height. According to their model, older and slower pulsars tend to have many emission heights, and a young pulsar like Vela would have a single emission height with about ten emission patches at that height. The consecutive bright pulses observed from Vela do not fit well with this model in its current form. From these observations, we would consider rejecting this model.

Kontorovich (2009) hypothesises that electromagnetic energy is trapped in the cavity between the neutron star surface and the magnetosphere. The standard pulse is this energy: “radiating through a ‘waveguide’ near the magnetic axis or through a ‘slot’ on the border of the open field lines”. Occasional breaks in the magnetosphere letting through this electromagnetic energy cause bright or giant pulses to be observed.

This inverts the traditional view in that the bright pulse reflects the normal state of the radiation field near the neutron star surface. The average pulse corresponds to strong attenuation through the magnetosphere. The observation that the consecutive bright pulses on Vela hold their phase position (before the main pulse) for several rotation periods indicates that these bright pulses are related to a specific part of the magnetosphere. Kontorovich's hypothesis is that these are gaps in the magnetosphere. But in this context, our observations would require that these gaps can remain open for a number of pulsar rotations.

Also of note is the fact that the last few pulses in the observation in Figure 34 are significantly lower in amplitude. This could be explained by the gap in the magnetosphere gradually closing.

Deshpande and Rankin (1999) study drifting sub-pulses in B0943+10 and produce a polar emission map showing, in a rotating frame, twenty emission centres around the magnetic axis. The pattern of emission centres takes 37 pulsar periods to complete one cycle around the magnetic axis. B0943+10 may provide a clue to the nature of the consecutive bright pulses observed in Vela, even though Vela does not have drifting sub-pulses. The period of B0943+10 is 1.098 s and the twenty emission centres are not tied to either the surface of the neutron star or to the magnetic field lines, and yet they remain stable over hundreds of seconds. If there is a virtually unseen analogue on Vela it could be hypothesised that it rotates an order of magnitude faster than the one on B0943+10 because Vela rotates an order of magnitude faster than B0943+10.

Krishnamohan and Downs (1983) break the pulse profile into 15 gates (depending on pulse flux density) and separately analyse the profile of each gate. The larger pulses have a single

peak that appears earlier. Our results confirm their observations. However, they also concluded that the pulse was made up of three (or four) components and that these components emit at different heights in the magnetosphere. The idea of different emission heights clashes with Karastergious and Johnston (2007), (because Vela should only have a single emission height) and it is also doesn't fit well with our observations of consecutive bright pulses.

However the multiple component aspect could be explained by Kontorovich's model if one or more components are the standard pulse energy radiating through a waveguide (or through a slot on the border of the open field lines), and the bright early component is a gap in the magnetosphere.

Combining the ideas proposed by Kontorovich and the stability and comparatively slow moving emission centres of Deshpande and Rankin, may lead to a refined emission model that explains the consecutive bright pulse observations reported here. The distribution of lifetimes of magnetospheric windows, or of emission columns, may follow from these results. Searches of other young pulsars for similar sequences of bright pulses would be very worthwhile, in order to determine whether Vela is peculiar or typical in showing this phenomenon.

8.2. Future Work

A list of questions that have come out of this research and some ideas for future study and observation.

- Search for consecutive bright pulses in other pulsars.
- Expand work on Vela glitches altering the rate of occurrence of bright pulses and consecutive bright pulses.
- Expand above to other pulsars.
- Is there a correlation of the above with pulsar age?
- Do bright pulses tie in with drifting sub pulses as observed by Deshpande and Rankin on B0943+10?
- Confirm whether giant micro pulses increase after a glitch in other pulsars.
- If so, can this be explained by any of the emission models?
- Can a glitch cause turbulence in the magnetosphere?
- Reconcile all the above with polarisation data.
- Observe consecutive bright pulses over a large frequency range, from different telescopes, simultaneously.
- Is there Fraunhofer diffraction occurring? Can this be modelled better?
- Does Vela actually have true Giants?

9.References

Abadie, J., et al*.,* 2011, ApJ 737, 93

Ables, J. G., McConnell, D., Deshpande, A. A., & Vivekanand, 1997, ApJ, 475, L33

Backer, D. C., Kulkarni, S. R., Heiles, C., Davis, M. M., & Goss, W. M., 1982, Nature, 300, 615

Buchner, S. 2010, The Astronomer's Telegram 2768,
http://www.astronomerstelegram.org/?read=2768

Cairns, I.H., Johnston, S., & Das, P. 2003, MNRAS 343, 512-522

Cordes, J. M., & Lazio, T. J. W., 2002, *NE2001. I. A New Model for the Galactic Distribution of Free Electrons and its Fluctuations*, arXiv:astro-ph/0207156

Cha, A. M., Sembach, K. R., & Danks, A. C. 1999, ApJ, 515, L25-L28

Deshpande, A. A., & Rankin, J. M. 1999, ApJ, 524, 1008-1013

Dodson, R., Lewis, L., & McCulloch, P., 2007, Astrophysics and Space Science, 308, 585-589

Edwards, R. T., & Stappers, B. W. 2002, A&A 393, 733-748

Hankins, T. H., & Eilek, J. A., 2007, Apj, 670, 693

Hewish, A., Bell, S. J., Pilkington, J. D. H., Scott, P. F., & Collins, R. A., 1968, Nature 217 (5130): 709–713, image downloaded from
http://www.cv.nrao.edu/course/astr534/images/PSRs_discovery.jpg

Hessels, J. W., Ransom, S. M., Stairs, I. H., Freire, P. C., Kaspi, V. M., & Camilo, F., 2006, Science 311 (5769), 1901–4.

Hotan, A. W., van Straten, W., & Manchester, R. N. 2004, PASA 21 (2004) 302-309

Hotan, A. W., 2006, PhD thesis, Swinburne University of Technology

Johnston, S., van Straten, W., Kramer, M., & Bailes, M. 2001, ApJ, 549:L101-L104

Kaspi, V. M. & Helfand, D. J., 2002, In: *Neutron Stars in Supernova Remnants*, p. 3, eds Slane P. O., & Gaensler, B. M., Astronomical Society of the Pacific, San Francisco

Karastergiou, A., & Johnston, S. 2007, MNRAS 380, 1678-1684

Karuppusamy, R., Stappers, B. W., & van Straten, W., 2010, Astronomy & Astrophysics, 515, A36

Kontorovich, V., M., 2009, *Proceedings of The 8th International Conference on Physics of Neutron Stars* in Saint-Petersburg, 2008, arXiv:0911.3272v2

Krishnamohan, S., & Downs, G. S., 1983, ApJ, 265, 372

Large, M. I., Vaughan, A. E., & Mills, B. Y., 1968, Nature 220, 340 - 341

Lattimer, J. M., & Prakash, M., 2001, ApJ, 550, 426

Link, B., Epstein, R.I., & van Riper, K.A., 1992, Nature 359, 616-618

Lorimer, D. R. & Kramer M. 2005, *Handbook of Pulsar Astronomy* (Cambridge University Press)

Lyne A. G., & Manchester, R. N. 1988, MNRAS, 234, 477

Manchester, R. N., Hobbs, G. B., Teoh, A., & Hobbs, M., AJ, 2005, 129, 1993-2006, http://www.atnf.csiro.au/people/pulsar/psrcat/

Michel, F., 1970, ApJ, 159, L25-L28

Mignani, R. P., Zharikov, S., & Caraveo, P. A., 2007, Astronomy & Astrophysics, 473, 891-896

Palfreyman, J. L., Hotan, A. W., Dickey, J. M., Young, T. G., Hotan, C. E., 2011, ApJ 735, L17

Pellizzoni, A., et al., 2009 ApJ 691, 1618

Pellizzoni, A., et al., 2010, Science, 327, 663-665

Poov, M. V. & Stappers, B., 2007, Astronomy & Astrophysics, 470, 1003

Pines D. & Alpar, M. A., 1985, Nature, 316, 27

Rankin, J. M., 1993, ApJ, 405, 285

Stairs, I. H., 2004, Science, 304, 547

van Straten, W. & Bailes, M., 2011, PASA, 28, 1-14

Vaughan, A. E., 2008, Orange Pulsar Presentation

Wallace, P. T., Peterson, B. A., Murdin, P. G., et al., 1977, Nature, 266, 692
